model for investigating the molecular basis of intrahepatic metastasis of HCCs, because it exerts a strong metastatic potential *in vivo*, with marked cell scattering *in vitro* compared to other hepatomas.[5,7] In a previous study, we found that *in vitro* culture of KYN-2 cells on integrin-stimulating cell-substrata significantly induced cell scattering, and the disruption of E-cadherin-mediated intercellular adhesion, suggesting that one of the main reason for invasive property of HCC is integrin signaling.[7] Integrin receptors are composed of α–β heterodimers that recognize extracellular matrices, which not only provide a link with the actin cytoskeleton, but also serve as signaling receptors affecting cell behavior and various types of gene expression.[8] It is widely accepted that altered levels in integrin expression are closely involved in gain of tumorigenesis and metastatic ability in cancer cells.[9–11] In human HCC, reduced expression of β integrin subunits α2, α3 and α5 and overexpression of subunit α6 were reported to be associated with increased aggressiveness.[12–14] Moreover, several *in vitro* experiments indicated that β1 integrin plays a critical role in the invasive phenotype of HCC cell lines.[15,16] Therefore, to understand the molecular basis of integrin signaling pathway in HCC, investigating its downstream intracellular signaling seems important. To date, however, there have been no reports, which examined intracellular signaling in HCC with regards to integrin-mediated invasive property.

It has been revealed that integrin-mediated extracellular signals stimulate a wide variety of intracellular signaling events including tyrosine phosphorylation,[17,18] calcium influx,[19] and activation of the mitogen-activated protein kinase family such as extracellular signal-regulated kinase (ERK)[20] and c-Jun NH2-terminal kinase.[21] Among these intracellular events, ERK signaling seems of value for investigation, because it was reported that activated ERK was frequently observed in human HCC tissues.[22] Although there have been no reports which examined the molecular relationship between ERK signaling and gain of invasive phenotype of HCC, it is worth noting that *in vitro* experiments had revealed that the ERK signaling pathway was involved in the migration of pancreatic cancer cells.[23] Therefore, to further understand the molecular mechanisms of intrahepatic metastasis of HCC, we investigated the biological potential of ERK signaling during integrin-stimulated cell scattering, using the highly metastatic HCC cell line KYN-2.

Materials and methods

Antibodies and Reagents

Mouse monoclonal antiphospho-p44/42 ERK1/2 (Thr202/Tyr204) E10 was purchased from Cell Signaling Technology (Beverly, MA, USA), and functional neutralizing mouse monoclonal antibody against β_1 integrin (P4C10) was obtained from Chemicon (Temecula, CA, USA). Rabbit polyclonal antihemagglutinin (HA) tag was from Clonetech (Palo Alto, CA, USA). Mouse monoclonal anti-ERK kinase (MEK) 1, anti-ERK1, anti-ERK2, and anti-c-Cbl were from Transduction Laboratories (Lexington, KY, USA). Mouse monoclonal anti-E-cadherin (HECD1) was from TaKaRa Shuzo (Siga, Japan). Mouse monoclonal anti-βactin (AC-15), polyhydroxyethylmethacrylate (poly-HEMA), poly-L-lysine (PLL) and tetramethyl rhodamine iso thiocyanate (TRITC)-labeled phalloidin were from Sigma Chemical (St Louis, MO, USA). MEK inhibitor PD98059 was from Upstate Biotechnology Inc. (Lake Placid, NY, USA), and the other MEK inhibitor U0126 was from Promega (Madison, WI, USA). Recombinant human epidermal growth factor (EGF) and hepatocyte growth factor (HGF) were from TOYOBO (Osaka, Japan).

Cell Culture

Human HCC cell line KYN-2 was kindly provided by Dr M Kojiro (Kurume University, Kurume, Japan).[24] To evaluate morphological changes of KYN-2 in response to cell–substratum adhesion, cells were cultured on the culture dishes with or without poly-HEMA-coating in RPMI-1640 medium containing antibiotics (100 U/ml penicillin and 100 μg/ml streptomycin) with or without 10% (v/v) fetal bovine serum. The culture dishes were made of anionic and hydrophilic polystyrene, which enables maintenance of cell adhesion through facilitating matrix deposition when serum is added to the culture media. Poly-HEMA is a nonionic material that blocks extracellular matrix deposition, and cell attachment irrespective of the presence of serum in the media. To investigate effects of growth factors or integrin/MEK signaling effectors on morphological changes in KYN-2 cells, cells were deprived of serum for 12 h to avoid serum-associated nonspecific stimulation; and then, cells were incubated with appropriate agents with the same media. EGF or HGF was added to the culture medium at a final concentration of 50or 40 ng/ml, respectively; and a neutralizing antibody of β_1 integrin P4C10 was added at a concentration of 20 μg/ml. MEK inhibitors PD98059 and U0126 were dissolved in dimethylsulfoxide (DMSO), and added to the culture medium at concentrations of 25 and 10 μM, respectively. After addition of each reagent to the culture medium, cellular morphological changes were observed at regular intervals for 48 h. Cell surface area was quantified by measuring randomly selected individual cells in several scanned photographs.

A calcium-dependent cell dissociation assay was performed as previously described.[25] Briefly, confluent monolayers were incubated with 0.01% (w/v) trypsin with or without 1.25 mM calcium at 37°C for 15 min. After addition of trypsin inhibitor, cells

were gently pipetted 10 times, and degree of cell dissociation was evaluated using a microscope.

Transfection Assay

MEK1 is known to be activated via phosphorylation of Ser218 and Ser222 residues, and substituting these two sites with aspartic acid can mimic phosphorylation, and lead to a constitutively active type.[26,27] To activate the MEK/ERK signaling pathway in KYN-2 cells, cells were transfected with MEK1 S218D/S222D mutant-containing pUSE plasmids (Upstate Biotechnology Inc., Lake Placid, NY, USA) using Superfect™ Transfection Reagents (QIAGEN, Hilden, Germany). Stable transfectants of active-MEK1 plasmids were selected using geneticin (G418; 400 μg/ml; GIBCO-BRL), screened for HA-tagged MEK1 expression by immunoblotting, and recloned. Control mock transfectants were transfected with empty pUSE plasmid vectors, and cloned in the same manner.

Immunoblotting

In all experiments, levels of expression and phosphorylation of ERK1 were analyzed 36 h after plating. Protein samples were extracted in lysis buffer (50 mM Tris pH 8.0, 150 mM sodium chloride, 1 mM sodium vanadate, 0.1% (v/v) sodium dodecyl sulfate, and 1% (v/v) Nonidet P-40) for 20 min at 4°C. Lysates were precleared by centrifugation, and protein concentration was determined using a Bradford assay (Bio-Rad Laboratories, Hercules, CA, USA). Proteins were electrophoresed on sodium dodecyl sulfate-polyacrylamide gels, and transferred to Immobilon membranes (Millipore, Bedford, MA, USA). After blocking nonspecific sites, filters were reacted with appropriate primary antibodies and corresponding horseradish peroxidase-conjugated secondary antibodies. Peroxidase-labeled bands were visualized using an enhanced chemiluminescence detection system (Amersham International, Buckinghamshire, UK).

Immunocytochemistry

For immunocytochemical analysis, cells were fixed with 4% (v/v) paraformaldehyde in phosphate-buffered saline (pH 7.4) containing 2% (w/v) sucrose, and permeabilized with 0.1% (v/v) Triton X-100. Cells were incubated with 2% (v/v) normal swine serum for blocking nonspecific reaction sites, reacted with appropriate primary antibodies at 4°C overnight, followed by incubation with the corresponding FITC-labeled secondary antibodies. Actin filaments were visualized using TRITC-labeled phalloidin. Immunostained cultured cells were mounted using Vectashield (Vector Laboratories, Burlingame, CA, USA), and examined using a Zeiss LSM410 confocal microscope (Carl Zeiss, Thornwood, NY, USA).

In Vitro Wound Healing Assay

Cells were plated on six-well plates at a density of 1×10^6 cells/plate, and cultured overnight in the presence of 10% (v/v) fetal bovine serum. When cells were grown to confluence, a linear wound of the monolayer was created by scratching with a pipette tip of a diameter of 1 mm. Morphology and migration of cells were observed, and photographed at regular intervals, and degree of cell motility was assessed as the ratio of the wound width between 0 and 48 h.

Antibody-Based Protein Microarray

To investigate downstream signaling molecules during integrin/MEK/ERK-mediated cell scattering, an antibody-based microarray assay was performed. Pairs of protein samples were obtained from KYN-2 cells cultured for 36 h on poly-HEMA and fibronectin-coated dishes, or from MEK2D and mock-transfected KYN-2 cells cultured for 36 h on uncoated plastic dishes. Cells were processed for Antibody Microarray™ (BD biosciences Clontech, Palo Alto, CA, USA) to assess expression profiles of 512 molecules (http//www.clontech.co.jp). Each of the paired protein samples was labeled with fluorescent dye Cy3 or Cy5, and was competitively hybridized on the same slide surface where 512 antibodies were spotted. Image analysis was performed using the Axon GenePix 4.1 software package (Axon Instruments, Foster City, CA, USA). Expression ratios of each molecule in the paired samples were normalized using an internal control according to the manufacturer's protocols, and internally normalized ratios <0.8 or above 1.8 were considered as being significant among samples.

Results

Morphological Changes of KYN-2 Cells in Response to Cell-Substratum Adhesion

When KYN-2 cells were cultured on poly-HEMA-coated dishes in the presence of serum, they did not adhere to the dishes, but floated in media, and tightly aggregated with each other (Figure 1a, upper left). In contrast, when KYN-2 cells were cultured on uncoated plastic dishes in the same conditioned culture media, they adhered on the plates and markedly scattered, showing weavy-protruded cell membranes (Figure 1a, upper right). Immunocytochemical analysis showed that actin filaments of KYN-2 cells plated on poly-HEMA were specifically localized in the area of cell-to-cell attachment like a honeycomb, which was similar to cortical actin bundles in differentiated epithelial cells (Figure 1a,

lower left). However, in cells adhered to culture dishes, actin filaments were distributed in the cytoplasm, and partially accumulated at the leading edge of ruffled cell membranes forming lamellipodia, which is characteristic of motile cells (Figure 1a, lower right).

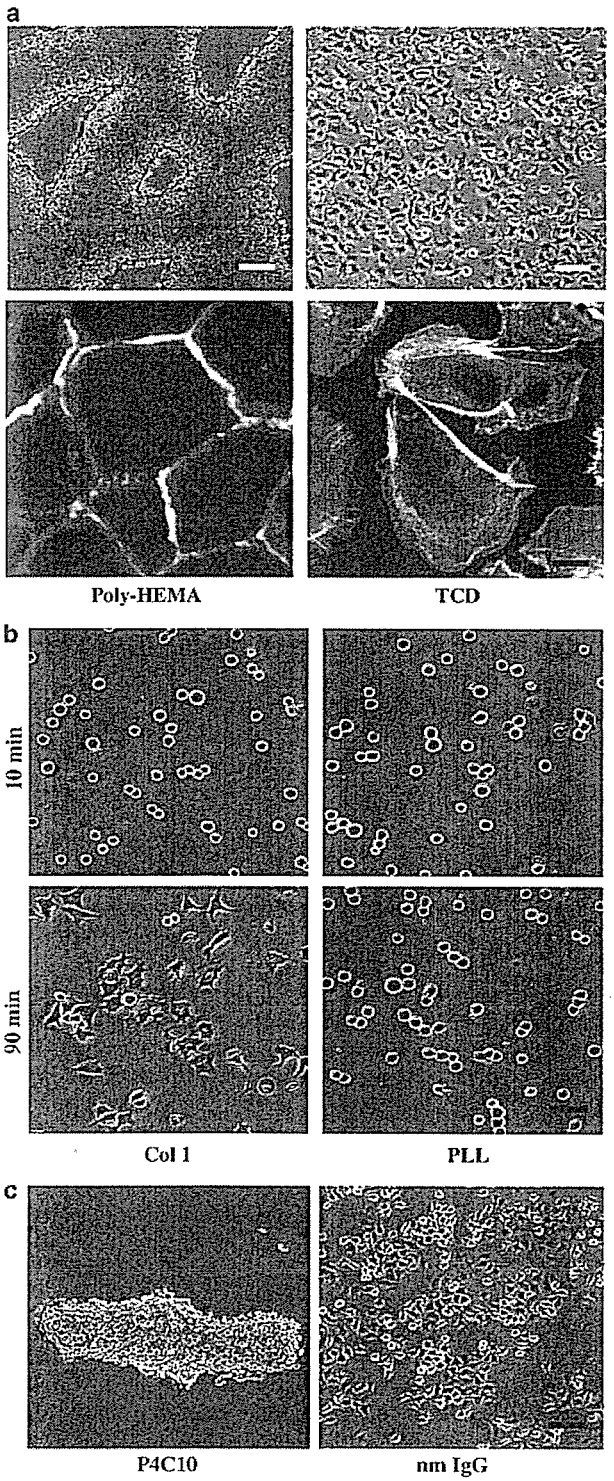

Cell Scattering of KYN-2 Cells is Mediated by Integrin-Stimulating Substratum

To investigate whether growth factors affected cell scattering in KYN-2 cells, EGF or HGF was added to the serum-free culture medium for blocking nonspecific integrin ligands. Neither EGF nor HGF affected degree of cell scattering in cells plated on uncoated and fibronectin (FN)- or type I collagen (Col I)-coated plastic dishes, indicating little involvement of these growth factors in morphologic changes of KYN-2 cells (data not shown).

To address the roles of integrins in cell–substratum-dependent morphological changes in KYN-2 cells, cells were plated on the dishes coated with either FN, Col I (both are specific ligands of integrins), or PLL (a positively-charged nonspecific adhesion-promoting polypeptide), and cultured in media deprived of serum. When KYN-2 cells were seeded on FN- or Col I-coated dishes, they adhered to plates within 10 min, and scattered over a period of 90 min, showing lamellipodia extension with membrane ruffles (Figure 1b, left column). On the other hand, when cells were seeded on PLL-coated dishes, they adhered to dishes but did not scatter (Figure 1b, right column). Shapes of cells plated on PLL remained unchanged, and lamellipodia extensions or membrane ruffles were never observed. When a neutralizing antibody against β_1 integrin P4C10 was added to the medium, cells plated on FN or Col I-coated dishes significantly aggregated with reduced scattering and decreased lamellipodia (Figure 1c). P4C10 also blocked scattering of cells plated on uncoated plastic dishes (data not shown), indicating that cell scattering of KYN-2 cells is mediated by integrin.

ERK is Phosphorylated through Integrin-Mediated Cell-Substratum Adhesion

To analyze the status of ERK signaling during integrin-elicited cell scattering, phosphorylated levels of ERK in KYN-2 cells in different conditions were analyzed by immunoblotting. There were no differences in total amounts of ERK1 (Figure 2a, bottom line) and ERK2 (data not shown) between cells plated on poly-HEMA-coated and uncoated

Figure 1 Morphological changes of KYN-2 cells with different substrata. (**a**) KYN-2 cells were cultured on the dishes with or without poly-HEMA-coating, in the presence of 10% (v/v) serum. Morphology was examined by phase-contrast microscopy (*upper*), and actin filaments were stained with TRITC-phalloidin (*lower*). (**b**) KYN-2 cells were cultured on dishes coated with type I collagen (col I) or poly-L-lysine (PLL) without serum, and photographed after 10 and 90 min. (**c**) Phase-contrast images of KYN-2 cells cultured on fibronectin-coated dishes with neutralizing monoclonal antibody against $\beta 1$ integrin (P4C10, *right*) and nonimmunized mouse IgG (nmIgG, *left*). *Scale bars:* 100 μm (**a**, *upper*, **b** and **c**), 5 μm (**a**, *lower*).

plastic dishes, in the presence of serum. However, phospho-ERK1/2 was markedly elevated in cells adhered to uncoated plastic dishes compared to cells cultured on poly-HEMA-coated dishes (Figure 2a, upper line). Increased levels of phospho-ERK1/2 were also observed in cells plated on FN- or Col I-coated plates, immediately after attachment to dishes (Figure 2b). However, cells plated on PLL did not show any phosphorylated ERK1/2 during culture maintenance (Figure 2b). P4C10 treatment significantly inhibited ERK1/2 phosphorylation in cells adhered to FN-coated plates (Figure 2c), indicating that blockade of $\beta 1$ integrin signaling prevented ERK phosphorylation.

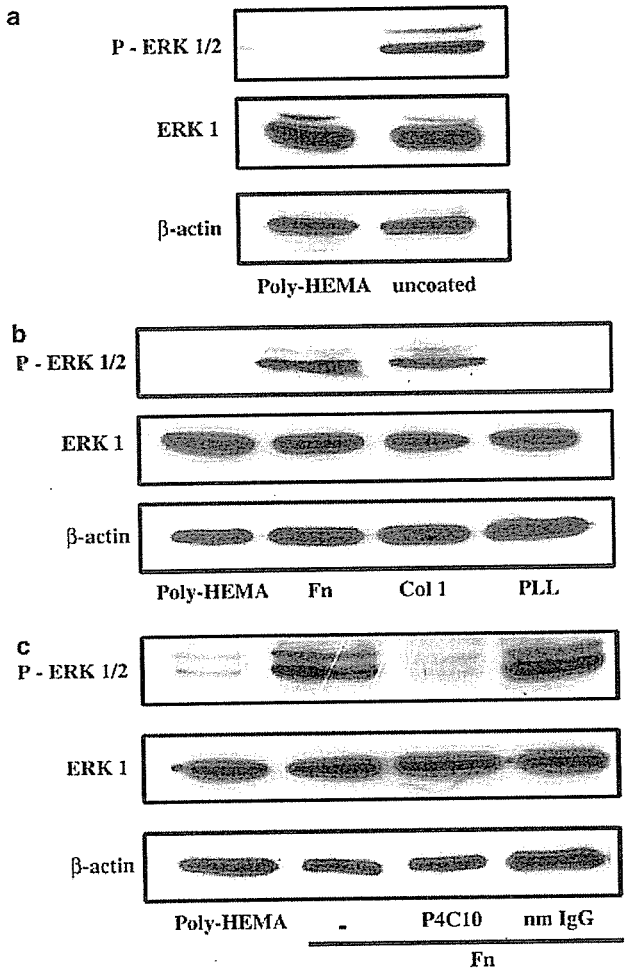

Figure 2 Immunoblotting of total and phosphorylated ERK. (**a**) KYN-2 cells were cultured on poly-HEMA coated dishes (poly-HEMA) or uncoated plastic dishes (uncoated), in the presence of 10% (v/v) serum. (**b**) Cells were cultured on dishes coated with poly-HEMA (poly-HEMA), fibronectin (Fn), type I collagen (I col) or poly-L-lysine (PLL) in serum-deprived medium. (**c**) Cells were cultured on dishes coated with poly-HEMA (poly-HEMA) or fibronectin (Fn), in the presence of nonimmunized mouse IgG (nmIgG) or neutralizing monoclonal antibody against $\beta 1$ integrin (P4C10).

Blockade of MEK-ERK Signaling Inhibits Cell Scattering of KYN-2 Cells

It is well known that activity of ERK is directly regulated by its upstream signaling mediator MEK.[28] Therefore, to comprehensively analyze the involvement of MEK-ERK signals in integrin-elicited cell scattering, MEK inhibitor PD98059 was added to KYN-2 cells plated on uncoated plastic dishes, in the presence of serum. Immunoblot analysis showed that levels of ERK1/2 phosphorylation were significantly reduced after treatment with PD98059, confirming that blockade of MEK signaling prevents ERK activity in KYN-2 cells (Figure 3a). Under phase-contrast microscopic examination, control DMSO-treated cells appeared to be of membrane-ruffled fusiform shape without tight cell-to-cell contact (Figure 3b, left upper column), which was the same as cells cultured on uncoated plastic dishes, as shown in Figure 1a. After treatment with PD98059 for 12 h, cells changed into a polygonal shape, decreased membrane ruffles, recovered tight cell–cell contact, and formed cohesive monolayer colonies (Figure 3b, right upper column). In control DMSO-treated cells, E-cadherin was diffusely expressed in the cytoplasm and faintly on cell membranes, but in PD98059-treated cells it was limited along with cell–cell contact areas (Figure 3b, middle column). Actin filaments were distributed in the cytoplasm, and accumulated at the ruffled cell membranes in DMSO-treated cells, whereas in PD98059-treated cells, they were mainly localized in the area of cell-to-cell attachment like cortical bundles (Figure 3b, bottom column).

MEK-ERK Signaling Cascade Induces Cell Spreading of KYN-2 Cells

To further gain insight into the roles of the MEK-ERK signaling cascade, we manipulated MEK1 activity in KYN-2 cells. Three clones of constitutively active MEK1 transfectants MEK2D-6, -8, -9, and two mock transfectants Mock 1 and 2 were obtained by stable transfection, and immunoblot analysis showed that all three MEK2D clones expressed an epitope-tagged active form of MEK1 (Figure 4, top column). All MEK2D clones showed significantly higher levels of phosphorylated ERK1/2 compared to those from the parent and mock transfectants, confirming that ERK was constitutively activated by MEK1 signaling in these clones (Figure 4). We first investigated whether enhanced MEK-ERK signaling affected cell shape of KYN-2 cells compared to cells plated on FN or Col I plates in our study. To avoid interference in cell shape and width by mutual neighboring cells, microscopic examination was performed at the time when cells were grown to sub-confluent densities. All three MEK2D clones cultured on uncoated plastic dishes showed broad lamellipodia with ruffling at edges of cell membranes, and exhibited marked somal

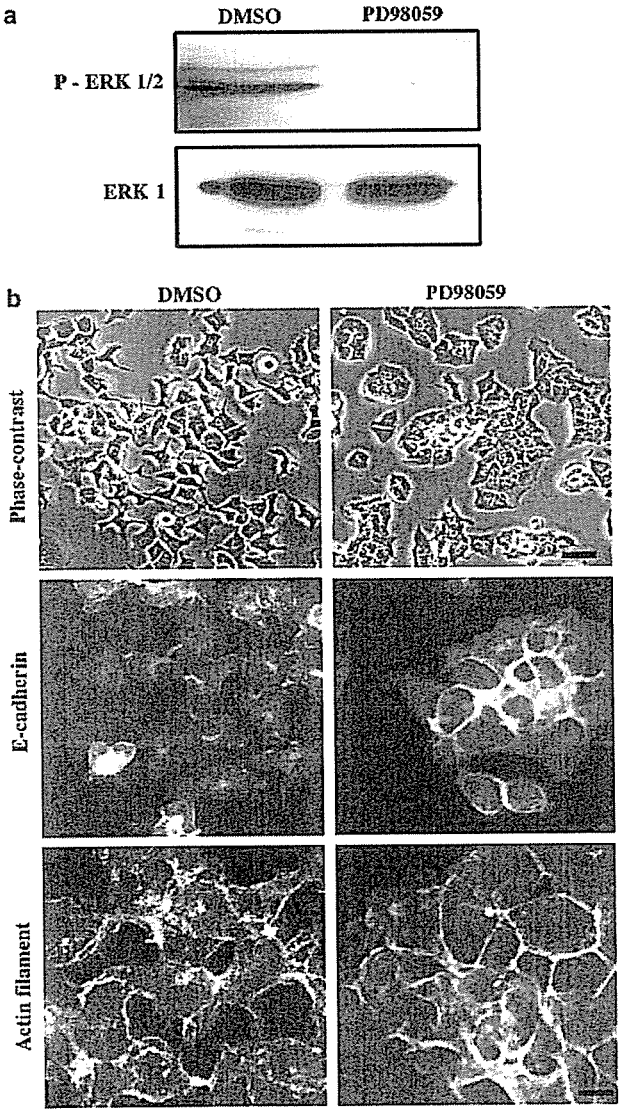

Figure 3 Effects of the MEK inhibitor PD98059 on KYN-2 cells. Cells were cultured on uncoated plastic dishes for 12 h in media containing 25 μM PD98059 dissolved in 0.002% (v/v) DMSO. Control cells were cultured with DMSO only. (**a**) Expressions of ERK1 and phosphorylated ERK1/2 in each sample were analyzed by immunoblotting. (**b**) Phase-contrast images (*upper*), confocal fluorescent images of E-cadherin (*middle*) and actin filaments (*lower*) in DMSO- or PDD98059-treated KYN-2 cells are shown. *Scale bars:* 20 μm (**b**, *upper*) 10 μm (**b**, *middle and lower*).

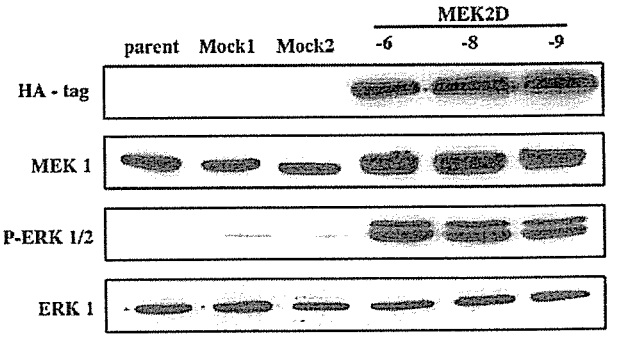

Figure 4 Immunoblotting of MEK1 in transfectants. Expressions of HA-tag, MEK1, phosphorylated ERK1/2 and ERK1 in each cell lysate of parent KYN-2 cells (parent), two control clones (mock1 and 2), and three clones expressing the constitutively active MEK1 mutant (MEK2D-6, -8, and -9) were analyzed by immunoblotting.

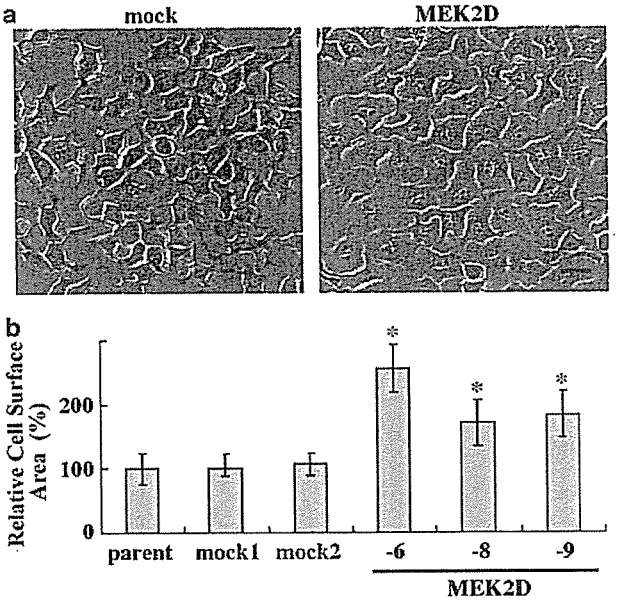

Figure 5 Morphological features of active MEK1 transfectants. (**a**) Phase-contrast view of mock cells (mock) and MEK2D clone 6 (MEK2D). Both cells were cultured in subconfluent densities on uncoated plastic dishes in the presence of 10% (v/v) serum. (**b**) Cell surface area was quantified by scanning photographic images of 100 individual randomly-selected cells. Each bar shows the ratio of the cell surface area of cells compared to those of parent cells. Data represent means$\pm$s.d. ($P<0.0001$; an asterisk shows significance as assessed by Student's *t*-test). *Scale bar:* 20 μm.

flattening compared to parent and mock transfectants (Figure 5a). Mean cell surface area in MEK2D was 1.8- to two-folds of that of parent cells and mock transfectants (Figure 5b), indicating that MEK activation specifically induced spreading phenotype.

MEK1 Activation Inhibits E-Cadherin-Mediated Cell-to-Cell Attachment

As we previously found that integrin-mediated spreading and migration of KYN-2 cells coincided with E-cadherin inactivation,[7] we examined whether cadherin-mediated cell–cell adhesion was influenced by MEK-ERK activation. Cells were grown to confluence to analyze the status of E-cadherin and actin filament in the area of cell–cell contact by immunocytochemistry. We found that E-cadherin expression in parent cells and mock transfectants was strong at the site of cell–cell contact, while was weak in MEK2D (Figure 5a, middle). Actin filaments in parent and mock transfectants were prominently localized at cell–cell contact sites like distinct cortical bundles, but were faint in the same area of MEK2D (Figure 5a, lower).

As E-cadherin expression was found to be weak in the area of cell–cell contact in MEK2D clones, a calcium-dependent dissociation assay was performed to investigate whether MEK-ERK signal influenced E-cadherin-mediated homotypic cell-to-cell adhesion. This assay is based on the mechanism that cultured adherent cells lose active cadherin, and are easily dissociated upon removal of calcium during trypsinization, but when calcium is added to the trypsin solution, cells hardly dissociate due to preserved cadherin function. In this assay, parent cells, mock transfectants and all MEK2D transfectants completely dissociated into single cells when calcium was deprived (Figure 6b, upper column). In the presence of calcium, parent cells and mock transfectants hardly dissociated during trypsinization. In contrast, MEK2D transfectants easily dissociated into single cells even in the presence of calcium (Figure 6b, lower column), indicating that enforced MEK-ERK signaling suppressed cadherin-mediated homotypic adhesion in KYN-2 cells.

MEK-ERK Signaling Cascade Induces Cell Motility in an *In Vitro* Wound Assay

To evaluate functional relationships between MEK-ERK signaling and cell motility in KYN-2 cells, *in vitro* wound assays were performed using active MEK1 transfectants. Within 48 h after scratching confluent cell layers, parent cells and mock transfectants had traversed to some extent but could not completely recover the wound of monolayered cells. However, all three MEK2D clones completely recovered the wound, and re-established a confluent monolayer during the same period (Figure 7a). Mean ratio of wound recovery was 70% in parent and mock transfectants, and 100% in MEK2D clones at 48 h, indicating a greater motility of the active MEK1 transfectants (Figure 7b).

C-Cbl is Downregulated during Integrin-MEK-ERK Signal-Induced Cell Scattering

To investigate mechanisms involved in integrin-MEK-ERK-induced hepatoma cell scattering, expression profiles of 512 signaling molecules (transcription factors, signaling mediators, cell cycle regulators, and cytoskeletal components, etc.) were analyzed using an antibody-based protein microarray. In all, 22 molecules showed significantly altered expression levels between KYN-2 cells plated on poly-HEMA-coated dishes and cells plated on fibronectin-plated dishes. Of these, similar expression profiles were observed for

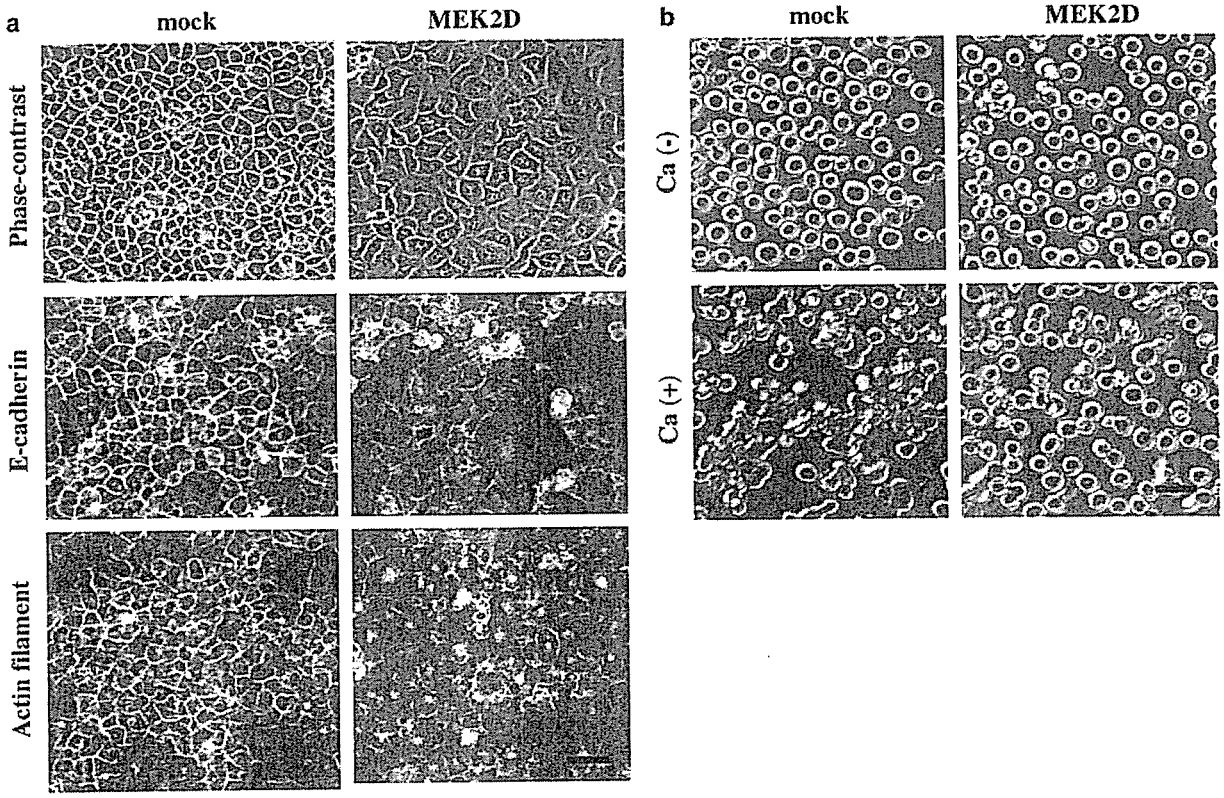

Figure 6 Reduced expression of E-cadherin and actin filaments in the area of cell-to-cell contact in active MEK1 transfectants. (a) Phase-contrast images (*upper*), confocal fluorescent images of E-cadherin (*middle*) and actin filaments (*lower*) of mock cells (*left*) and MEK2D clone 6 (*right*) grown to confluence on the uncoated plastic dishes. (b) Confluent cultured monolayer cells were treated with 0.01% (w/v) trypsin at 37°C for 15 min without (*upper*) or with (*lower*) 1.25 mM calcium. *Scale bar*: 50 μm.

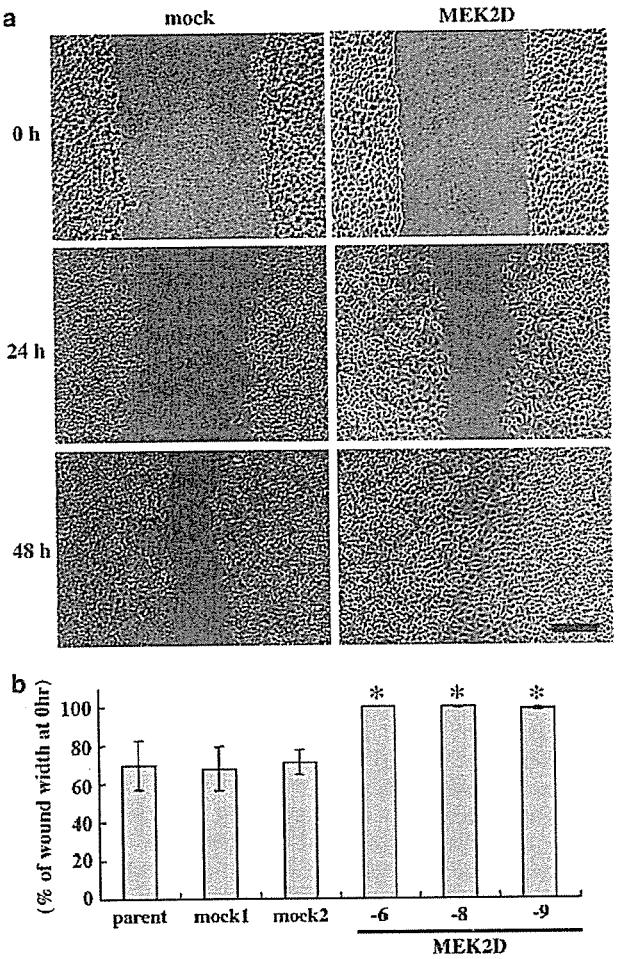

Figure 7 Increased motility of active MEK1 transfectants as assessed by an *in vitro* wound assay. (**a**) Phase-contrast images of mock transfectants (mock) and MEK2D clone 6 (MEK2D) are shown. Indicated times (0, 24, and 48 h) depict the duration after scratching of the monolayer. (**b**) Each bar shows the ratio of the wound width between before and after 48 h of scratching. Data represent means ± s.d. ($P<0.0001$, an asterisk shows significance compared to parent cells using a Student's *t*-test). Three experiments were independently performed in the assay. Scale bar 200 μm.

13 molecules between MEK2D-transfected KYN-2 and mock-transfected cells (Table 1). Among these candidates, immunoblot analysis confirmed that c-Cbl was significantly downregulated in MEK2D transfectants compared to control mock transfectants and parent cells (Figure 8). Densitometry analysis showed that c-Cbl expression was reduced by about 90% in MEK2D transfectants compared to controls.

Discussion

Cancer metastasis is generally considered to be a multistep process, that is, it involves (1) cell detachment and scattering from a primary tumor, (2) migration into the stroma, (3) entry into the vascular and/or lymphatic system, (4) dispersal through the circulation, and (5) proliferation in the seeded organ. Aggressive cancer phenotypes may have properties to complete all these steps,[29] because each step seems to be a requisite for metastatic behaviors. In HCC, portal invasion and intrahepatic metastasis are frequently observed in cases with infiltrative cancer growth into the surrounding liver at the periphery of tumors,[4] and gain of migration ability of HCC cells *in vitro* is considered to reflect their intrahepatic metastatic potential *in vivo*.[5,6] Therefore, the initial steps of cancer metastasis including detachment of cancer cells from the primary lesion and scattering to surrounding tissues, may offer the best target to regulate intrahepatic metastatic ability of HCC cells.

To precisely investigate molecular mechanisms of cell-to-cell detachment and scattering of HCC, we used the human HCC-derived cell line KYN-2 which

Table 1 Antibody microarray analysis

Antigen name	*Accession No.*	*Expression ratio (INR)*	
		FN vs *HEMA*	*MEK2D* vs *Mock*
Upregulated by integrin/MEK signaling			
CD28	P10747	2.42	1.91
Downregulated by integrin/MEK signaling			
BTF	Q9NYF8	0.34	0.68
NuMA	Q14980	0.49	0.58
C-NAPI	O60588	0.38	0.40
NF-kB	Q04206	0.51	0.51
TNIK	Q9UKE5	0.47	0.62
c-Cbl	P22681	0.50	0.64
Cdk7	P50613	0.42	0.50
Ezrin	P15311	0.52	0.52
Pericentrin	P48725	0.39	0.72
MONA	O75791	0.45	0.39
Perforin	P14222	0.52	0.68
BART	Q9Y2Y0	0.44	0.72

Representative results of antibody-based microarray analysis of paired samples from KYN-2 cells cultured on fibronectin (FN) *vs* poly-HEMA (HEMA)-coated dishes, and from MEK2D-transfectants (MEK2D) *vs* mock controls (Mock). The internally normalized ratio (INR) of paired samples was over 1.00 when expression increased in cells plated on FN-coated dishes or in MEK2D transfectants.

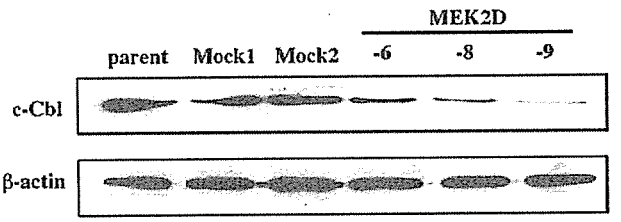

Figure 8 C-Cbl expression is downregulated in active MEK1 transfectants. Expressions of c-Cbl and β actin in KYN-2 parent cells (parent), control clones (mock1 and 2), and clones constitutively expressing active MEK1 mutants (MEK2D-6, -8, and -9) were analyzed by immunoblotting.

has a high propensity for intrahepatic metastasis *in vivo* and shows high migration ability *in vitro*.[5] Our results showed that KYN-2 cells float as trabecular structures with tight cell aggregation when suspended on poly-HEMA-coated dishes. In contrast, when KYN-2 cells were cultured on the dishes in the presence of serum or on collagen type 1 or fibronectin-coated dishes without serum, both of which conditions were under integrin-mediated stimulation, they dissociated from each other, and significantly scattered. These morphological changes were not found in the presence of EGF and HGF, and were effectively inhibited by addition of a neutralizing antibody against $\beta 1$ integrin. Therefore, scattering ability of KYN-2 cells may be exclusively regulated by integrin signaling. In this study, we found a close relationship between intracellular ERK signaling and integrin-elicited morphological changes in this HCC cell line. Immunoblot analysis showed that phosphorylated levels of ERK were significantly increased when KYN-2 cells showed scattering on the dishes with serum or on integrin-stimulating substrata such as collagen type 1 and fibronectin. Conversely, P4C10 treatment prevented phosphorylation of ERK in these cells.

ERK is known to be activated via phosphorylation by MEK signaling.[27] Therefore, to investigate the role of MEK-ERK signaling cascade in integrin-elicited cell scattering and morphological changes in KYN-2, we examined effects of PD98059 which inhibits ERK phosphorylation through the blockade of MEK activity.[30] Our results showed that PD98059 efficiently blocked cell dissociation, and induced the formation of cohesive colonies of cells plated on the uncoated plastic dishes, in the presence of serum. E-cadherin and actin filaments were predominantly accumulated in the area of cell–cell contact in these cells. Treatment with another MEK inhibitor U0126 resulted in similar results (data not shown), therefore MEK-ERK signaling cascade may be a requisite for integrin-elicited scattering in KYN-2 cells. Our *in vitro* wound assay may support this idea, showing that cell motility increased in active MEK1-transfectants. To further understand the significance of integrin-MEK-ERK signaling in the metastatic potential of hepatoma cells, additional studies using several methodological approaches (eg, *in vitro* trans-well migration assay, and *in vivo* mouse model using orthotopic transplantation) should be performed.

In normal epithelial cells, cell-to-cell adhesion is mainly mediated by E-cadherin in a calcium-dependent homophilic manner, which is thought to act as an 'invasion suppressor system' in cancer cells.[31] E-cadherin exerts a signaling linkage signal between extracellular matrices and the actin cytoskeleton through catenins, and promotes cell-to-cell adherence,[32] thereby preventing cell detachment and scattering. Our present study suggested that MEK-ERK signaling cascade dominated E-cadherin-mediated cell adhesion, as cadherin-mediated homotypic adhesion was abrogated in active MEK1 transfectants in a calcium-dependent cell dissociation assay. A similar finding of the relationship between activated ERK and adherence junction disassembly was recently reported in Ras-transformed or hepatocyte growth factor-stimulated Mardin-Darby canine kidney cells.[33] However, there have been no studies which examined the correlation of cadherin with integrin-MEK-ERK signaling. To our knowledge, this is the first study to show that integrin-MEK-ERK-mediated cell scattering resists E-cadherin-mediated cell–cell adhesion signal in metastatic cancer cells.

Downstream mechanisms of integrin-MEK-ERK-induced hepatoma cell scattering are intriguing. We analyzed expression profiles in KYN-2 cells using an antibody-based protein microarray, and found that the proto-oncogene product c-Cbl was significantly reduced when plated on FN or transfected constitutively active MEK gene. Several studies reported that c-Cbl acted as a negative regulator of cell motility by inhibiting membrane ruffles in NIH 3T3 fibroblasts,[34] and by ubiquitinating the Rho family guanine nucleotide exchange factor Vav in 293T embryonic kidney epithelial cells.[35] Our data may provide other insights in the mechanisms of c-Cbl-mediated cell scattering, by showing that c-Cbl was downregulated during integrin/MEK/ERK signaling-induced cell scattering in a highly metastatic hepatoma. It should be noted that c-Cbl acted as a negative regulator of EGF signaling by ubiquitinating EGFR, and inhibition of c-Cbl function is known to result in sustained activation of EGFR/ERK signaling.[36] Therefore, together with our data, in a highly metastatic hepatoma KYN-2, downregulation of c-Cbl by integrin/MEK/ERK signaling might result in sustained activation of intrinsic EGFR signaling which enables a positive feedback of EGFR/MEK/ERK signaling to reinforce cell scattering. Further studies should be performed to better understand the biological significance of c-Cbl in hepatoma cell scattering.

Recently, a close relationship between MEK-ERK signaling and cell proliferation in HCC tissues was reported.[37,38] As our data showed that MEK-ERK signaling played a critical role in motility of the invasive HCC cell line KYN-2, this intracellular signaling may not only result in cell proliferation, but also deeply contribute to the first steps of metastasis of HCC. We suggest that blockade of integrin-MEK-ERK pathway may provide a useful therapeutic approach to prevent intrahepatic metastasis of human HCC.

References

1 Nagao T, Inoue S, Goto S, *et al.* Hepatic resection for hepatocellular carcinoma. Clinical features and long-term prognosis. Ann Surg 1987;205:33–40.

2 Nagáo T, Inoue S, Yoshimi F, *et al.* Postoperative recurrence of hepatocellular carcinoma. Ann Surg 1990;211:28–33.
3 Nakashima T. Vascular changes and hemodynamics in hepatocellular carcinoma. In: Okuda K, Peter RL (eds). Hepatocellular Carcinoma. Wiley: New York, 1976, pp 169–203.
4 Kanai T, Hirohashi S, Upton MP, *et al.* Pathology of small hepatocellular carcinoma. A proposal for a new gross classification. Cancer 1987;60:810–819.
5 Genda T, Sakamoto M, Ichida T, *et al.* Cell motility mediated by Rho and Rho-associated protein kinase plays a critical role in intrahepatic metastasis of human hepatocellular carcinoma. Hepatology 1999;30: 1027–1036.
6 Takamura M, Sakamoto M, Genda T, *et al.* Inhibition of intrahepatic metastasis of human hepatocellular carcinoma by Rho-associated protein kinase inhibitor Y-27632. Hepatology 2001;33:577–581.
7 Genda T, Sakamoto M, Ichida T, *et al.* Loss of cell-cell contact is induced by integrin-mediated cell-substratum adhesion in highly motile and highly-metastatic hepatocellular carcinoma cells. Lab Invest 2000;80: 387–394.
8 Juliano RL, Haskill S. Signal transduction from the extracellular matrix. J Cell Biol 1993;120:577–585.
9 Plantefaber LC, Hynes RO. Changes in integrin receptors on oncogenically transformed cells. Cell 1989;56: 281–290.
10 Giancotti FG, Ruoslahti E. Elevated levels of the $\alpha5\beta1$ fibronectin receptor suppress the transformed phenotype of Chinese hamster ovary cells. Cell 1990;60: 849–859.
11 Dedhar S, Saulnier R, Nagle R, *et al.* Specific alterations in the expression $\alpha3\beta1$ and $\alpha6\beta4$ integrins in highly invasive and metastatic variants of human prostate carcinoma cells selected by *in vitro* invasion through reconstituted basement membrane. Clin Exp Metastasis 1993;11:391–400.
12 Jaskiewicz K, Chasen MR. Differential expression of transforming growth factor α, adhesions molecules and integrins in primary, metastatic liver tumors and liver cirrhosis. Anticancer Res 1995;15:559–562.
13 Yao M, Zhou XD, Zha XL, *et al.* Expression of the integrin $\alpha5$ subunit and its mediated cell adhesion in hepatocellular carcinoma. J Cancer Res Clin Oncol 1997;123:435–440.
14 Begum NA, Mori M, Matumata T, *et al.* Differential display and integrin $\alpha6$ messenger RNA overexpression in hepetocellular carcinoma. Hepatology 1995;22: 1447–1455.
15 Matsumoto A, Arao S, Otsuki M. Role of $\beta1$ integrin in adhesion and invasion of hepatocellular carcinoma cells. Hepatology 1999;29:68–74.
16 Carloni V, Mazzocca A, Pantaleo P, *et al.* The integrin $\alpha6\beta1$ is necessary for the matrix-dependent activation of FAK and MAP kinase and the migration of human hepatocarcinoma cells. Hepatology 2001;34:42–49.
17 Clark EA, Brugge JS. Integrins and signal transduction pathways: the road taken. Science 1995;268:233–239.
18 Schwartz MA, Schaller MD, Ginsberg MH. Integrins: emerging paradigms of signaltransduction. Annu Rev Cell Dev Biol 1995;11:549–599.
19 Schwartz MA. Spreading of human endothelial cells on fibronectin or vitronectin triggers elevation of intracellular free calcium. J Cell Biol 1993;120:1003–1010.
20 Chen Q, Kinch MS, Lin TH, *et al.* Integrin-mediated cell adhesion activates mitogen-activated protein kinases. J Biol Chem 1994;269:26602–26605.
21 Miyamoto S, Teramoto H, Çosa OA, *et al.* Integrin function: molecular hierarchies of cytoskeletal and signaling molecules. J Cell Biol 1995;131:791–805.
22 Ito Y, Sasaki Y, Horimoto M, *et al.* Activation of mitogen-activated protein kinases/extracellular signal-regulated kinases in human hepatocellular carcinoma. Hepatology 1998;27:951–958.
23 Klemke RL, Cai S, Giannini AL, *et al.* Regulation of cell motility by mitogen-activated protein kinase. J Cell Biol 1997;137:481–492.
24 Yano H, Maruiwa M, Murakami T, *et al.* A new human pleomorphic hepatocellular carcinoma cell line, KYN-2. Acta Pathol Jpn 1988;38:953–966.
25 Nagafuchi A, Ishihara S, Tsukita S. The roles of catenins in the cadherin-mediated cell adhesion: functional analysis of E-cadherin-α catenin fusion molecules. J Cell Biol 1994;127:235–245.
26 Yan M, Templeton DJ. Identification of 2 serine residues of MEK-1 that are differentially phosphorylated during activation by raf and MEK kinase. J Biol Chem 1994;269:19067–19073.
27 Catling AD, Schaeffer HJ, Reuter CW, *et al.* A proline-rich sequence unique to MEK1 and MEK2 is required for raf binding and regulates MEK function. Mol Cell Biol 1995;15:5214–5225.
28 Crews CM, Alessandrini A, Erkinson RL. The primary structure of MEK, a protein kinase that phosphorylates the ERK gene product. Science 1992;258:478–480.
29 Poste G, Fidler IJ. The pathogenesis of cancer metastasis. Nature 1980;283:139–146.
30 Dudley DT, Pang L, Decker SJ, *et al.* A synthetic inhibitor of the mitogen-activated protein kinase cascade. Proc Natl Acad Sci USA 1995;92:7686–7689.
31 Hirohashi S. Inactivation of the E-cadherin-mediated cell adhesion system in human cancers. Am J Pathol 1998;153:333–339.
32 Nagafuchi A, Takeichi M. Cell binding function of E-cadherin is regulated by the cytoplasmic domain. EMBO J 1988;7:3679–3684.
33 Potempa S, Ridley AJ. Activation of both MAP kinase and phosphatidylinositide 3-kinase by Ras is required for hepatocyte growth factor/scatter factor-induced adherens junction disassembly. Mol Biol Cell 1998;9:2185–2200.
34 Scaife RM, Courtneidge SA, Langdon WY. The multi-adaptor proto-oncoprotein Cbl is a key regulator of Rac and actin assembly. J Cell Sci 2003;116: 463–473.
35 Miura-Shimura U, Duan L, Rao NL, *et al.* Cbl-mediated ubiquitinylation and negative regulation of Vav. J Biol Chem 2003;278:38495–38504.
36 Wu WJ, Tu S, Cerione RA. Activated Cdc42 sequesters c-Cbl and prevents EGF receptor degradation. Cell 2003;114:715–725.
37 Huynh H, Nguyen TT, Chow KH, *et al.* Over-expression of the mitogen-activated protein kinase (MAPK) kinase (MEK)-MAPK in hepatocellular cartcinoma: its role in tumor progression and apoptosis. BMC Gastroenterol 2003;3:19.
38 Tsuboi Y, Ichida T, Sugitani S, *et al.* Overexpression of extracellular signal-regulated protein kinase (ERK) and its correlation with proliferation in human hepatocellular carcinoma. Liver Int 2004;24:432–436.

THE JOURNAL OF GENE MEDICINE
J Gene Med 2006; 8: 623–635.
Published online 14 February 2006 in Wiley InterScience (www.interscience.wiley.com). **DOI:** 10.1002/jgm.880

RESEARCH ARTICLE

Attenuation of mouse acute colitis by naked hepatocyte growth factor gene transfer into the liver

Takayasu Hanawa[1]
Kenji Suzuki[1]*
Yusuke Kawauchi[1]
Masaaki Takamura[1]
Hiroyuki Yoneyama[4]
Gi Dong Han[2]
Hiroshi Kawachi[2]
Fujio Shimizu[2]
Hitoshi Asakura[1]
Jun-ichi Miyazaki[5]
Hiroki Maruyama[3]
Yutaka Aoyagi[1]

[1]*Department of Gastroenterology and Hepatology*

[2]*Department of Cell Biology, Institute of Nephrology*

[3]*Department Clinical Nephrology and Rheumatology, Niigata University Graduate School of Medical and Dental Sciences, Niigata City, Niigata, Japan*

[4]*Department of Molecular Preventive Medicine, University of Tokyo Graduate School of Medicine, Bunkyo-ku, Tokyo, Japan*

[5]*Division of Stem Cell Regulation Research, Osaka University Graduate School of Medicine, Suita, Osaka, Japan*

*Correspondence to: Kenji Suzuki, Department of Gastroenterology and Hepatology, Niigata University Graduate School of Medical and Dental Sciences, 1-757 Asahimachi-dori, Niigata City 951-8510, Japan.
E-mail: kjsuzuki@med.niigata-u.ac.jp

Received: 20 May 2005
Revised: 24 November 2005
Accepted: 25 November 2005

Abstract

Background Hepatocyte growth factor (HGF) has multiple biological effects on a wide variety of cells. It modulates intestinal epithelial proliferation and migration, and critically regulates intestinal wound healing.

Aims To investigate the therapeutic effect of HGF gene transfer, we introduced the HGF gene into the liver of mice with acute colitis.

Methods The rat HGF expression plasmid vector, pCAGGS-HGF, was injected via the tail vein into C57BL/6 mice, followed by dosing with dextran sulfate sodium in distilled water. Firstly, the HGF gene was injected once on day 0. Secondly, the HGF gene was injected on day 0 and again on day 2.

Results Injection of the HGF gene ameliorated colitis with inhibition of both loss of body weight and shortening of colon length. It protected the colon from epithelial erosions and cellular infiltration. Expression of mRNAs for IFN-γ, IL18, and TNF-α was reduced in the colon. In contrast, expression of mRNA for IL-10 was increased. The numbers of BrdU-positive intestinal epithelial cells were increased, and the numbers of TUNEL-positive apoptotic cells were decreased. Furthermore, a second injection prolonged the elevation of serum HGF levels, and ameliorated the symptoms better than a single injection. The empty pCAGGS plasmid did not ameliorate acute colitis.

Conclusions HGF gene transfer attenuated acute colitis by facilitating intestinal wound repair as well as inhibiting inflammation, suggesting a new strategy for treatment of IBD.

Keywords HGF; c-Met; inflammatory bowel disease; DSS colitis; naked gene transfer

Introduction

Inflammatory bowel disease, which comprises ulcerative colitis and Crohn's disease, is characterized by chronically relapsing inflammation of the bowel of unknown origin [1]. Therapy for inflammatory bowel disease has been aimed predominantly at the regulation of the inflammatory cells and their production of various inflammatory mediators, such as arachidonic acid metabolites, chemokines, and pro-inflammatory cytokines [2,3]. Conventional therapy for inflammatory bowel disease involves 5-aminosalicylates, corticosteroids, and immunosuppressive drugs such as azathioprine. Tumor necrosis factor (TNF)-α and interleukin (IL)-6 have been investigated as target molecules for the development of newer therapeutic approaches for inflammatory bowel disease [4]. Anti-TNF-α antibodies have been established

for the treatment of Crohn's disease [5], and anti-IL-6 receptor antibodies have been tried clinically with great success [6]. These agents are beneficial and established as a standard therapy for inflammatory bowel disease; however, they have limited response rate and serious side effects. Therefore, newer therapeutic approaches are required.

Epidermal growth factor (EGF) is a potent mitogenic peptide produced by the salivary and duodenal Brunner's glands and stimulates several components of the healing response [7,8]. In a recent report, EGF enema has been shown to be an effective treatment for active left-sided ulcerative colitis [9]. Thus, newer therapeutic approaches for inflammatory bowel disease should be aimed at regeneration and repair of the wounded intestinal epithelial cells of the bowel as well as inhibition of inflammation.

Hepatocyte growth factor (HGF) is a pleiotropic factor initially identified as a growth factor for hepatocytes [10–12]. It has mitogenic, motogenic, and morphogenic functions in various types of cells, including gastrointestinal epithelial cells [13–15], through its high-affinity receptor tyrosine kinase, Met, that is encoded by the c-*met* proto-oncogene [16]. HGF activator, HGF activator inhibitor type-1, and HGF-associated molecules involved in the activation of HGF in injured tissues are associated with colonic mucosal repair [17]. HGF expression has been reported to be up-regulated in the inflamed colonic mucosal tissue in patients with ulcerative colitis [18], and plasma HGF levels are increased in animal models of acute colitis [19]. Recently, the administration of recombinant human HGF has been shown to facilitate colonic mucosal repair in rats with dextran sulfate sodium (DSS)-induced colitis [20], and in HLA-B27 transgenic rats [21].

Liver is an important target organ for gene transfer because of its high capacity for synthesizing serum proteins and its involvement in numerous genetic and acquired diseases [22]. Among the various gene delivery systems available, naked DNA-mediated gene transfer is the simplest, and techniques for introducing DNA into hepatocytes have been the most intensely studied methods for generating therapeutic amounts of gene product [23]. High levels of foreign gene expression can be achieved in mouse hepatocytes by rapid tail vein injection of a large volume of naked DNA solution, the 'hydrodynamics-based procedure' [24]. In this study, we investigated the therapeutic effect of rat HGF gene transfer into the liver by the hydrodynamics-based method in a murine model of colitis.

Materials and methods

Animals and induction of colitis

Female C57BL/6 (B6) mice (7–8 weeks old) were purchased from Charles River Japan (Atsugi, Kanagawa, Japan) and maintained in the Animal Center of Niigata University School of Medicine under specific pathogen-free conditions. Colitis was induced in the mice by the administration of 3–5% DSS (molecular weight 36 000–50 000; Wako, Osaka, Japan) in distilled water *ad libitum* for 7 days. Three hours before the administration of DSS at day 0 and/or day 2, we injected HGF or control vector into the mice as described below. Body weight, stool consistency (scores: 0, normal stools; 1, soft stools; 2, liquid stools), hemoccult positivity and the presence of gross blood (scores: 0, negative fecal occult blood; 1, positive fecal occult blood; 2, visible rectal bleeding) were assessed daily. The disease activity index (DAI) was determined as a combination of the above parameters according to the scoring criteria as we described previously [25]. All animal experiments were performed according to the 'Guide for Animal Experiments' of Niigata University School of Medicine.

Plasmid DNA injection techniques

Plasmid pCAGGS-rat-HGF was constructed by inserting the rat HGF cDNA into a unique EcoRI site in the pCAGGS expression vector, which has the CAG (cytomegalovirus immediate-early enhancer/chicken β-actin hybrid) promoter, and grown in *Escherichia coli* DH5α (Toyobo, Osaka, Japan). The plasmid was prepared using a Qiagen Endofree plasmid Giga kit (Qiagen GmbH, Hilden, Germany), as described previously. The empty pCAGGS plasmid was used as a control. The plasmid DNA was diluted in 2 ml (approximately 1/10 of the body weight) of Ringer's solution (Ohtsuka, Tokushima, Japan) at room temperature. At day 0 and/or day 2, we anesthetized the mice with diethyl ether, and injected 10 μg of either pCAGGS-HGF or pCAGGS plasmid into the tail vein through a 27-gauge needle with a <3 s injection time.

Measurement of HGF in plasma

To determine the concentration of HGF at various time points after injection, we used an enzyme-linked immunosorbent assay (ELISA) kit for rat HGF (Institute of Immunology, Tokyo, Japan) including an antibody that cross reacts with mouse HGF. Values are expressed in ng/ml.

Evaluation of histology

The degree of colonic injury was assessed by colon length and histological score. The entire colons (10 mice per group) were sampled and their lengths were recorded immediately. The entire colon was fixed in 4% formalin, embedded in paraffin, and transverse sections were stained with hematoxylin and eosin. According to the preliminary histological interpretation, we analyzed the distal colon tissue section located approximately 10 mm from the anal verge to calculate the number of infiltrating

cells in the lamina propria of the colon. The crypt length of the colon of each mouse was also calculated as a mean value of five different crypts.

Quantitative reverse-transcription polymerase chain reaction (RT-PCR) to detect cytokine mRNAs

Total RNA was extracted from colon specimens with Trizol (Gibco BRL) according to the standard protocol then reverse-transcribed. Thereafter, cDNA was amplified using the ABI 7700 sequence-detector system (Applied Biosystems, Foster City, CA, USA) with a set of primers and probes corresponding to IFN-γ, TNF-α, IL-1β, IL-12, IL-18, IL-4, IL-10, and glyceraldehyde-3-phosphate dehydrogenase (GAPDH), as described previously.

X-gal and immunohistochemical staining

pCAGGS-lacZ expresses *E. coli* β-galactosidase. The lung, heart, liver, spleen, and kidneys were harvested for X-gal staining 1 day after the injection of 10 μg of pCAGGS-lacZ, embedded in Tissue-Tek OCT compound (Sakura Finetechnical Co. Ltd., Tokyo, Japan), and then frozen in a mixture of dry ice and acetone. Serial sections (5-μm thick) were cut with a cryostat and placed on glass slides coated with 3-aminopropyltriethoxysilane. Then the sections were fixed in 1.5% glutaraldehyde at room temperature for 10 min, washed three times in cold phosphate-buffered saline (PBS) (5 min/wash), and incubated in an X-gal staining solution containing 1 mg/ml X-gal, 2 mM $MgCl_2$, 5 mM $K_4Fe(CN)_6$, 5 mM $K_3Fe(CN)_6$, and 0.5% Nonidet P-40 in PBS, pH 7.4, at 37 °C for 3 h, followed by counterstaining with nuclear fast red.

Immunohistochemical staining

All mice were injected with BrdU (Sigma) (500 μg/100 μl in PBS) 1 h before killing. To detect replicating cells, tissue sections were reacted with the antibody and reagents using a BrdU staining kit (ZYMED, South San Francisco, CA, USA) according to the manufacturer's instructions. Crypts that had five or more BrdU-labeled nuclei were defined as surviving crypts. The numbers of BrdU-labeled nuclei of colonic epithelial cells for each group were compared.

Terminal deoxynucleotide transferase labeling

Apoptotic cells were identified using an *in situ* apoptosis detection kit (Takara Biomedicals, Japan) according to the manufacturer's instructions. In brief, acetone-fixed 5-mm fresh-frozen colon sections were permeabilized on ice and incubated with the terminal deoxynucleotide transferase mixture for 1 h at 37 °C. FITC-labeled dNTP were treated with anti-FITC HRP for 30 min, visualized with DAB, and counterstained with hematoxylin.

Monoclonal antibodies

The following monoclonal antibodies were used for immunofluorescence and flow cytometric analyses: anti-CD4 (clone GK1.5, IgG2b), anti-CD8 (clone 53-6.7, IgG2a), anti-B220 (clone RA3-6B2, IgG2a), anti-Mac-1 (clone M-70.15, IgG2b), anti-mouse INF-γ (clone XMG1.2), and anti-mouse IL-10 (clone JES5-16E3).

For immunostaining of HGF and c-Met, a goat polyclonal IgG antibody raised against a peptide mapping at the carboxyl terminus of HGFα (C-20; Santa Cruz Biotechnology, Santa Cruz, CA, USA) or an affinity purified rabbit polyclonal antibody raised against a peptide mapping at the carboxyl terminus of c-Met p140 of mouse origin (SP260; Santa Cruz Biotechnology) was used.

IF staining procedure

Frozen sections of the colon were prepared in a cryostat and stained with several fluorescent dye-conjugated anti-mouse antibodies as described above. The sections were observed by fluorescence microscopy.

Ex vivo colonic tissue culture

Ex vivo colon tissue culture was done by the established method with modification described as below [26]. The entire colon was taken from B6 mice with DSS colitis on days 2 and 5, or from those without colitis. The left side of the colon was cut into small pieces, each of which weighed 15 mg. Each colon sample was washed three times using RPMI 1640 culture medium containing 10% FBS (fetal bovine serum), penicillin G (100 IU/ml), and streptomycin (10 ng/ml), and placed in a center well of an organ culture dish (Falcon; Becton Dickinson Labware, NJ, USA). The center well of the dish was filled with 1 ml of the same medium, and incubated for 2 h and 24 h at 37 °C under 95% air and 5% CO_2. To evaluate the direct effect of HGF on *ex vivo* colon tissue, each sample was treated with recombinant human HGF (IBL, Gunma, Japan) at a concentration of 10 ng/ml at the beginning of tissue culture. The total RNA was extracted from each colon tissue and analyzed as described above for determining the mRNA expression levels for IFN-γ, IL-10, mouse HGF, and c-Met.

Statistical analysis

Data are expressed as means ± standard deviation (SD). Statistical analyses were performed using the unpaired

Student's t test or the nonparametric Mann-Whitney test. Differences were considered significant at $p < 0.05$.

Results

Localization of pCAGGS-lacZ gene expression and serum levels of rat HGF after pCAGGS-HGF injection

To clarify the site of transgene expression, we delivered 10 μg of pCAGGS-lacZ or pCAGGS into the tail vein of normal mice. LacZ gene expression was assessed in various organs including the liver, heart, lungs, kidney, spleen, and colon. X-gal stained only in the liver of the pCAGGS-lacZ-injected mice (Figure 1A), but not in the liver of the pCAGGS-injected mice (data not shown). The stained cells were predominantly hepatocytes, which were identifiable by their polygonal shape and round nuclei, visible at a higher magnification. We did not find convincing examples of X-gal-stained cells in the heart, lungs, kidney, spleen, or colon of the pCAGGS-lacZ-injected mice (data not shown).

We also confirmed the expression of HGF in hepatocytes in the liver of mice 2 days after injection of 10 μg pCAGGS-HGF by immunofluorescence using anti-HGF antibody (Figure 1C). Expression of HGF was not detected in the liver of mice injected with pCAGGS (Figure 1D). In the liver of mice injected with pCAGGS-HGF, the expression levels of rat HGF mRNA were significantly increased, but these were not increased in mice injected with control pCAGGS (data not shown).

We next evaluated the time course of rat HGF expression after the injection of 10 μg of DNA, using a less than 3-s injection time and a volume of 2 ml. Mice were injected with either 10 μg of pCAGGS-HGF ($n = 5$) or 10 μg of pCAGGS ($n = 5$). After injection of pCAGGS-HGF, the peak plasma HGF level was 15 ± 5 ng/ml at 12 h; then it decreased gradually, and became undetectable at 60 h (Figure 1B). The plasma rat HGF levels in the control mice were not significantly increased (Figure 1B).

HGF and c-Met expression after pCAGGS-HGF injection in the colons of mice with DSS colitis

Administration of DSS did not change the time course of the plasma rat HGF level after either pCAGGS or pCAGGS-HGF injection. In other words, after injection of pCAGGS-HGF into mice with DSS colitis, the peak plasma HGF levels were at 15 ng/ml at 12 h, and then decreased gradually and became undetectable at 72 h. The plasma rat HGF levels were not significantly increased in the DSS colitis mice injected with the empty pCAGGS.

Next we evaluated the expression of HGF and c-Met in colon tissues of mice with DSS colitis by immunofluorescence at day 2 after gene transfer. HGF expression was not detected in the colons of mice injected with either pCAGGS or pCAGGS-HGF. In contrast, c-Met expression was detected in epithelial cells of the crypts of the colons of both groups (Figures 1E and 1F). The number of c-Met-positive epithelial cells was greater in pCAGGS-gene transferred mice, and stronger expression was detected in the epithelial cells of the apical side of the crypt.

HGF gene transfer protected mice from DSS colitis

To determine the effect of HGF gene transfer on colon injury, we injected 10 μg of pCAGGS-HGF or pCAGGS into the tail veins of mice before DSS administration. Mice injected with control vector pCAGGS showed 10–20% weight loss, together with diarrhea, and gross bleeding; however, pCAGGS-HGF injection ameliorated clinical disease severity from day 1 to day 4 (Figure 2A). The decrease in colon length reflects the extent of colon damage in the model, and it was minimal in mice with HGF gene transfer at days 2, 5, and 6 compared with the mice injected with control vector (Figure 2B).

In mice injected with pCAGGS, broad mucosal ulceration and degeneration, and inflammatory cellular infiltration were observed, and these lesions progressed with time (Figures 2C–2I). Inflammatory cells were infiltrated to the colon progressively with time in mice with DSS colitis which were injected with pCAGGS; however, pCAGGS-HGF injection significantly reduced the number of inflammatory cells in the colon of mice with DSS colitis (Figure 2J).

The crypt length was decreased in colitis mice injected with pCAGGS. In contrast, HGF gene transfer prevented the shortening of crypt in DSS colitis (Figure 2K).

The effect of HGF gene transfer on immune cell trafficking into the colon of DSS colitis

An immunofluorescence study revealed that DSS-induced mucosal inflammation was accompanied by a significant infiltration of Mac-1+ macrophages, CD4+ T cells, CD8+ T cells, and B220+ cells in the lamina propria of mice injected with the empty pCAGGS (Figures 3A–3D, 3I).The numbers of these immune cells were significantly reduced in mice after HGF gene therapy (Figures 3E–H, 3I).

The effect of HGF gene transfer on cytokine mRNA expression in the colons of mice with DSS colitis

To reveal the immune response in the colon of mice with DSS colitis, we analyzed the expression of mRNA of several cytokines. At day 2 after induction of colitis, the levels of expression of the mRNAs for proinflammatory

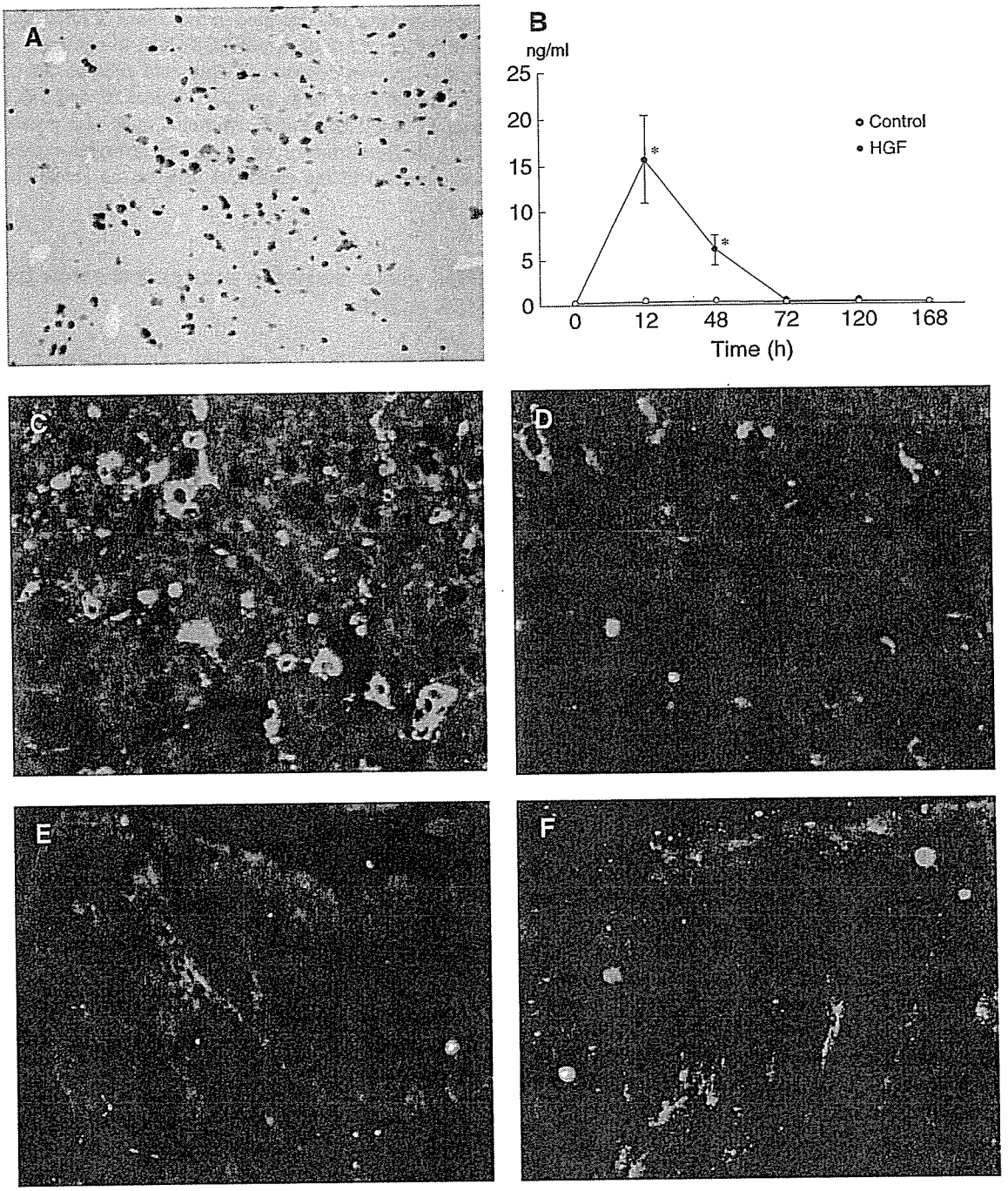

Figure 1. HGF gene transfection into the liver elevated serum HGF in mice. (A) X-gal-stained mouse liver section 1 day after injection with pCAGGS-lacZ. Original magnification: ×30. (B) Plasma levels of HGF at various time points. Blood samples were collected at 12, 48, 72, 120, and 168 h after pCAGGS-HGF injection following administration of DSS, and were detected by polyclonal HGF ELISA. Data are expressed as mean (SD), n = 10. *$p < 0.01$ versus control. (C) HGF expression was detected by immunofluorescence in the livers of mice with DSS colitis, which were injected with pCAGGS-HGF. (D) HGF was not detected by immunofluorescence in control, pCAGGS-injected mice. (E, F) c-Met, the receptor for HGF, was detected on colonic epithelial cells of mice with DSS colitis by immunofluorescence, and its expression was elevated slightly in mice injected with pCAGGS-HGF (E) compared with pCAGGS-injected mice (F)

cytokines such as IL1-β, IL18, and IFN-γ were increased, and those of TNF-α were increased at day 6 (Figure 3J). HGF gene transfer clearly reduced the expression of mRNAs for these cytokines (Figure 3K). Expression of IL-4 mRNA was increased slightly, but there was no statistical difference between mice injected with pCAGGS and those with pCAGGS-HGF (Figure 3K). Interestingly, expression of mRNA of IL-10, which is known to be an anti-inflammatory cytokine, was increased markedly at day 6 in the colons of both groups of mice; however,

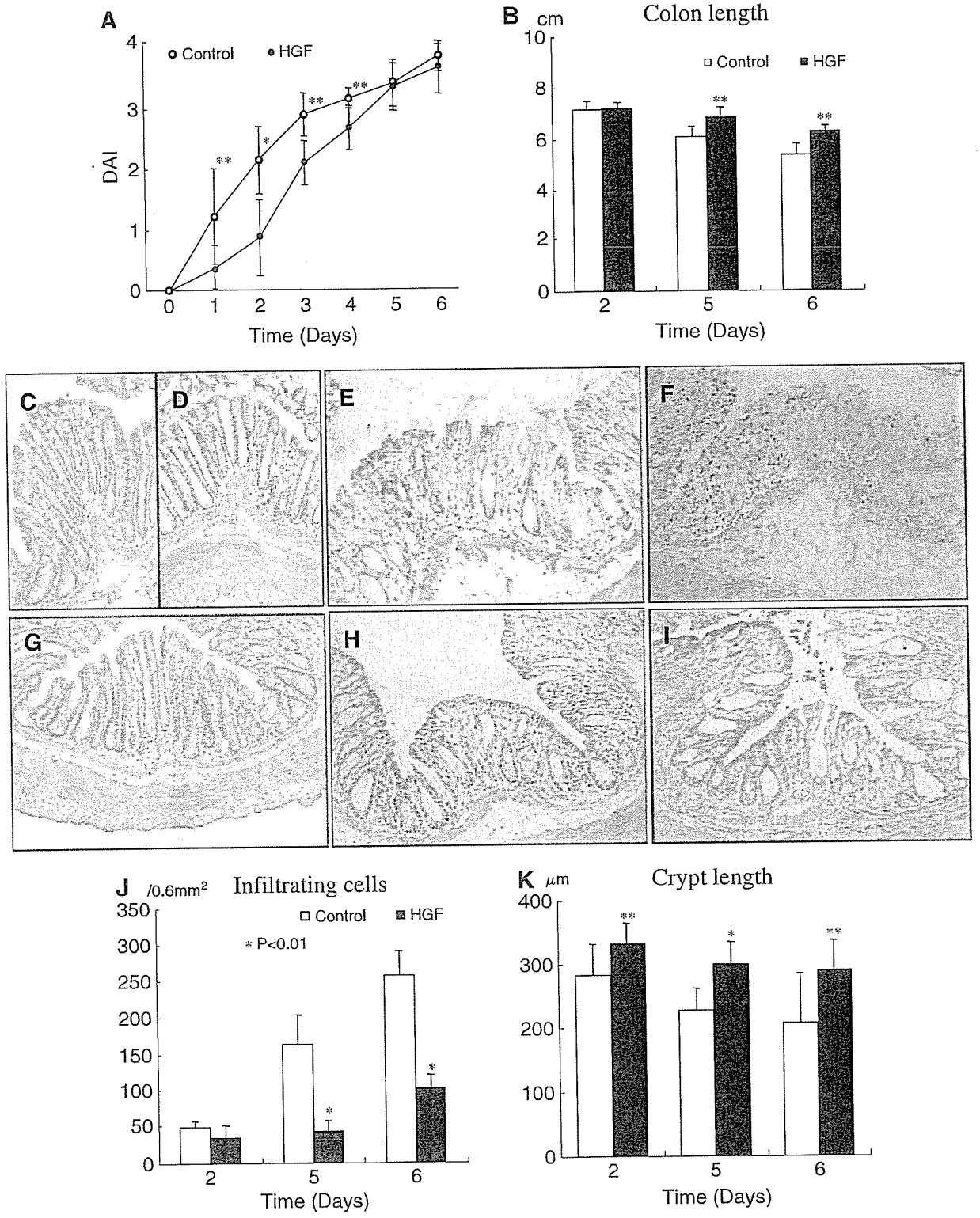

Figure 2. HGF gene transfer protected mice from acute colitis induced by DSS. (A) Disease activity index (DAI). Open circles, control pCAGGS-injected mice; closed circles, pCAGGS-HGF-injected mice. (B) Colon length, at days 2, 5, and 6. Open bars, control-pCAGGS; closed bars, pCAGGS-HGF. (C–I) Distal colon tissues: (C) from a normal mouse; (D) from pCAGGS-injected mice on day 2, (E) day 5, (F) and day 6 after DSS; and from pCAGGS-HGF-injected mice on day 2 (G), day 5 (H), and (I) day 6 after DSS. (J–K) Histological scores of colitic lesions. (J) The number of infiltrating cells in the lamina propria of the colon, at days 2, 5, and 6 after DSS. Open bars, from pCAGGS-injected mice; closed bars, pCAGGS-HGF-injected mice. (K) The crypt length of colon of mice, at days 2, 5, and 6 after DSS. Open bars, from pCAGGS-injected mice; closed bars, pCAGGS-HGF-injected mice. *$p < 0.01$; **$p < 0.05$

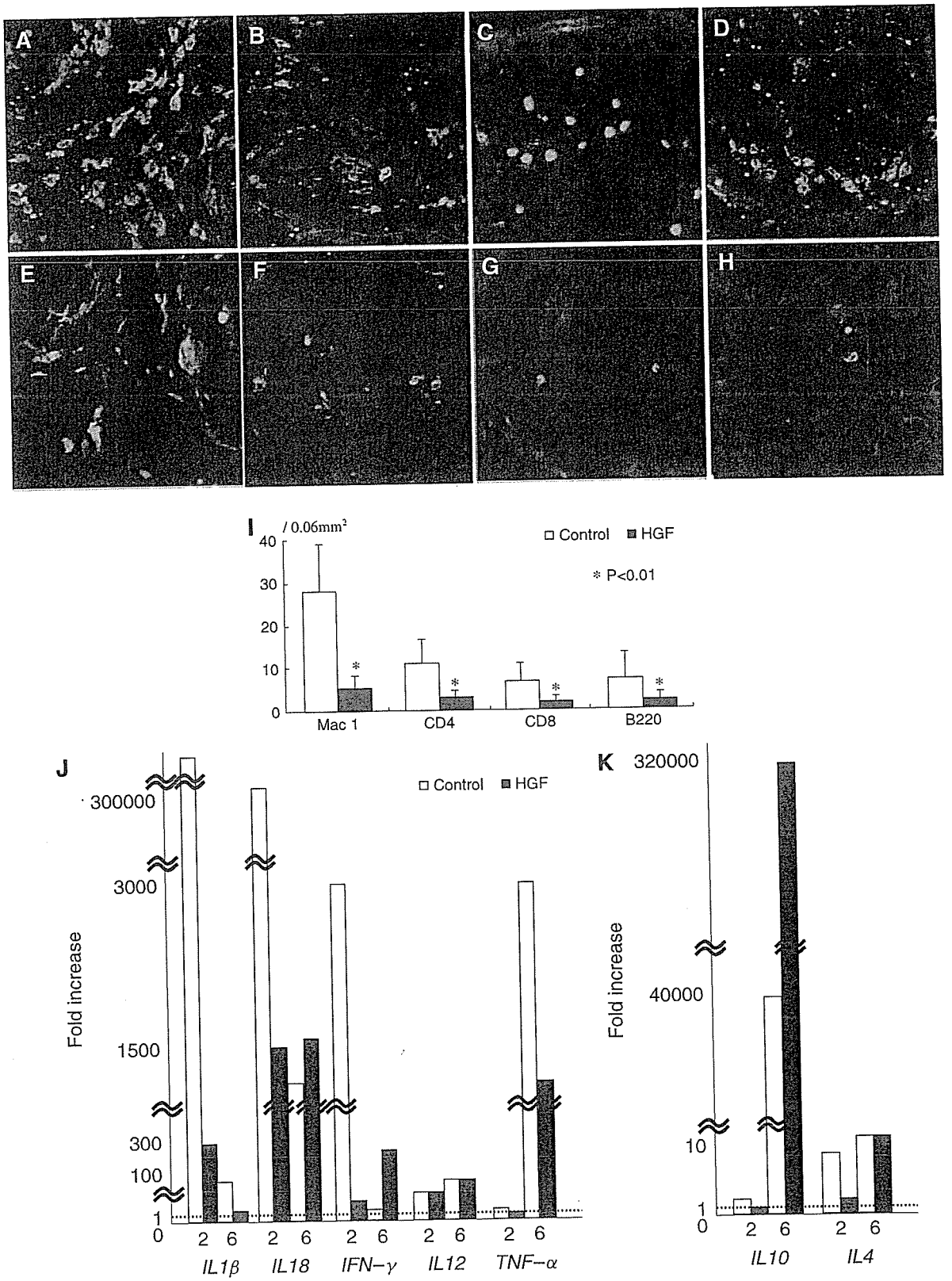

Figure 3. HGF transfection into the liver blocked immune cell traffic into the colon. (A–H) Immunostaining for Mac-1 (A, E), CD4 (B, F), CD8 (C, G), and B220 (D, H) of the distal colon tissues from pCAGGS-injected mice (A–D), and pCAGGS-HGF-injected mice (E–H). (I) Quantitative analysis of immune cells that infiltrated the colon. *$p < 0.01$. (J, K) Real-time quantitative PCR of pro-inflammatory and anti-inflammatory cytokines mRNA expression in the colon tissue. Open bars, from pCAGGS-injected mice; closed bars, pCAGGS-HGF-injected mice. Each amount was normalized to the level of GAPDH and the final relative values were expressed relative to the calibrators on day 0

HGF gene therapy significantly increased the expression level of IL-10 mRNA compared with the control vector (Figure 3K).

HGF gene transfer enhanced the proliferation of crypt epithelial cells in DSS colitis

We assessed the BrdU incorporation to evaluate the mitogenic effect of HGF on colonic epithelial cells in the amelioration of DSS colitis. BrdU+ cells were detected at the basal side of a crypt in the colon of mice with DSS colitis (Figures 4A and 4B); however, their numbers were much greater in mice that received HGF gene therapy than that of control vector (Figure 4C).

HGF gene transfer protected colonic mucosa from apoptosis in DSS colitis

As we have reported previously, apoptosis was observed in the colonic epithelial cells of mice with DSS colitis. HGF has an anti-apoptotic activity on several cells, and therefore we assessed the apoptotic epithelial cells in the colons of mice with DSS colitis using the terminal transferase uridyl nick endlabeling (TUNEL) method to detect DNA fragmentation *in situ*. TUNEL-positive colonic epithelial cells were observed along the crypts (Figures 4D and 4E), but their numbers were significantly reduced in mice that were transferred the HGF gene in comparison with that in control vector transferred mice (Figures 4D–4F).

Repeated injection of pCAGGS-HGF maintained peak levels of serum HGF longer and enabled a better cure of DSS colitis by facilitating regeneration and inhibiting apoptosis of crypt epithelial cells

Although HGF gene therapy could ameliorate acute colitis as described above, the benefit of the therapy is limited. The level of serum HGF is elevated within 3 days of a single injection of pCAGGS-HGF, and we speculated that maintenance of the elevated HGF level could induce a better therapeutic effect on colitis. We next injected pCAGGS-HGF twice, and the serum HGF level reached a peak at 12 h after the first gene injection, and decreased slightly, but was maintained at a level of 8 ng/ml during day 2 and day 5 after a second administration, 48 h after the first injection (Figure 5).

Clinical scores such as the DAI and the colon length of mice with DSS colitis were significantly ameliorated with the repeated HGF gene transfer compared to a single time administration (Figures 6A and B). Histologically, repeated injection of the HGF gene ameliorated the colitic lesions better than a single injection (Figures 6C–6F).

The numbers of BrdU-positive epithelial cells in the crypts of the colons were greater in mice injected with HGF twice than that of single injection (Figures 7A–7C). The

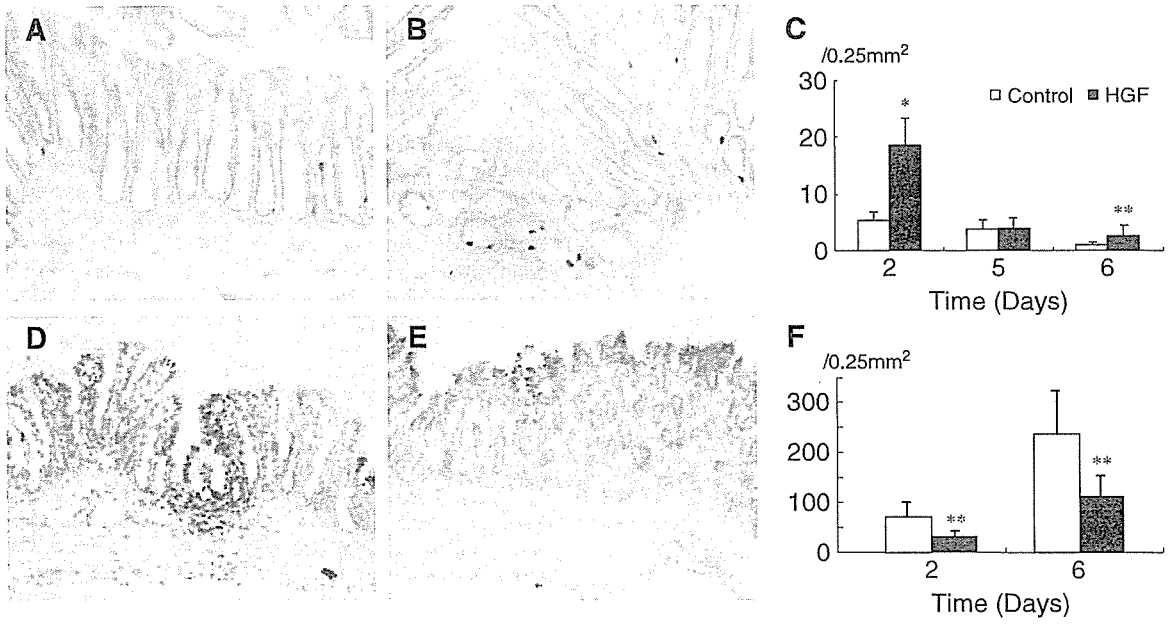

Figure 4. HGF gene transfection into the liver promoted proliferation and inhibited apoptosis of epithelial cells of the colon. (A–C) BrdU staining of distal-colon tissues from pCAGGS-injected mice (A), and pCAGGS-HGF-injected mice (B) at day 2 after DSS administration. The number of BrdU+ colonic epithelial cells (C). Open bars, from pCAGGS-injected mice; closed bars, pCAGGS-HGF-injected mice. (D–F) TUNEL staining of the distal colon tissues from pCAGGS-injected mice (D), and pCAGGS-HGF-injected mice (E) at day 2 after DSS administration. The number of TUNEL-positive apoptotic colonic epithelial cells (F). Open bars, from pCAGGS-injected mice; closed bars, pCAGGS-HGF-injected mice. $^{*}p < 0.01$; $^{**}p < 0.05$

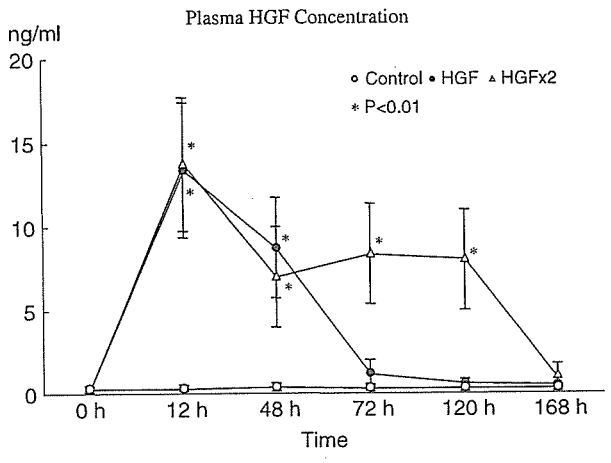

Figure 5. Repeated injection of pCAGGS-HGF kept the elevated level of plasma HGF. Plasma levels of HGF at various time points. Blood samples were collected at 12, 48, 72, 120, and 168 h after the first pCAGGS-HGF injection, and were detected by polyclonal HGF ELISA. pCAGGS-HGF was injected at 0 and 48 h after DSS administration. Open circles, pCAGGS-injected mice; closed circles, pCAGGS-HGF-injected once on day 0; open triangles, pCAGGS-HGF was injected on days 0 and 2 after DSS administration. Data are expressed as mean (SD), n = 10. *$p < 0.05$ versus control

number of TUNEL-positive apoptotic colonic epithelial cells was also reduced markedly in mice injected twice compared with mice with a single injection (Figures 7D–F).

The effect of HGF on cytokine mRNA expression in the colonic explants of mice with DSS colitis

To reveal the direct effect of HGF on immune response in the colon, we analyzed the expression of mRNA of IFN-γ and IL-10 in the colonic explants of mice with DSS colitis. In explants from mice with DSS colitis at days 2 and 5, the levels of expression of the mRNA of IFN-γ, a pro-inflammatory cytokine, was increased (Figure 8). The expression of mRNA of IFN-γ was clearly reduced by the treatment with HGF on explants (Figure 8). Expression of mRNA of IL-10, which is a known anti-inflammatory cytokine, was increased markedly at days 2 and 5 in the *ex vivo* colon tissue cultured with HGF (Figure 8). Interestingly, the expression of mRNAs for intrinsic mouse HGF and c-Met was clearly increased in explants cultured with HGF (Figure 8).

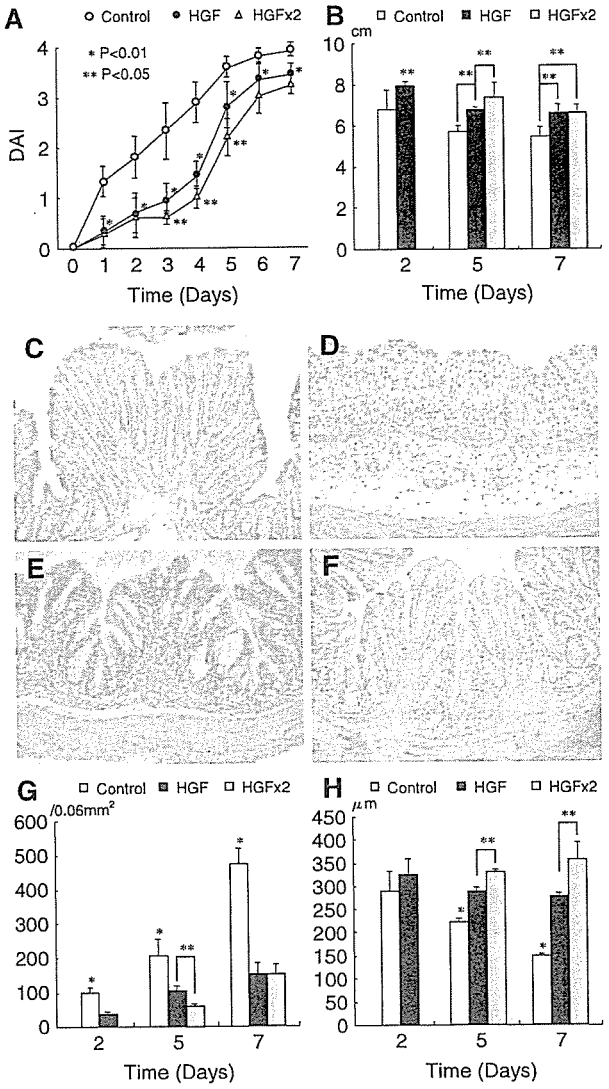

Figure 6. Repeated HGF gene transfer protected mice better from acute colitis induced by DSS. (A) Disease activity index (DAI). Open circles, control pCAGGS-injected mice; closed circles, pCAGGS-HGF-injected mice; open triangles, pCAGGS-HGF was injected on days 0 and 2 after DSS administration. (B) Colon length, at days 2, 5, and 7. Open bars, control pCAGGS; closed bars, pCAGGS-HGF; gray bars, pCAGGS-HGF was repeatedly injected on day 0 and day 2 after DSS administration. (C–F) Distal colon tissues: from a normal mouse (C); from pCAGGS-injected mice on day 2 after DSS (D); from mice with pCAGGS-HGF injection once on day 0 (E); and from mice with pCAGGS-HGF injections on days 0 and 2 (F). (G, H) Histological scores of colitic lesions. (G) The numbers of infiltrating cells in the lamina propria of the colon on day 6 after DSS. Open bars, control-pCAGGS; closed bars, pCAGGS-HGF; gray bars, pCAGGS-HGF was injected on day 0 and day 2 after DSS administration. (H) The crypt length of colons of mice on days 2, 5, and 6 after DSS. Open bars, control-pCAGGS; closed bars, pCAGGS-HGF; gray bars, pCAGGS-HGF was injected on days 0 and 2 after DSS administration. *$p < 0.01$; **$p < 0.05$

Discussion

There are various gene delivery systems, and the most intensely studied methods utilize viral vectors. There are concerns about the possibility of recombination with endogenous virus to produce a deleteriously infectious form. It has also been reported that T-cell leukemia developed nearly 3 years after gene therapy for SCID using a defective retroviral vector [27,28]. Thus, there are several hurdles to overcome to enable the clinical application of gene therapy with viral vectors.

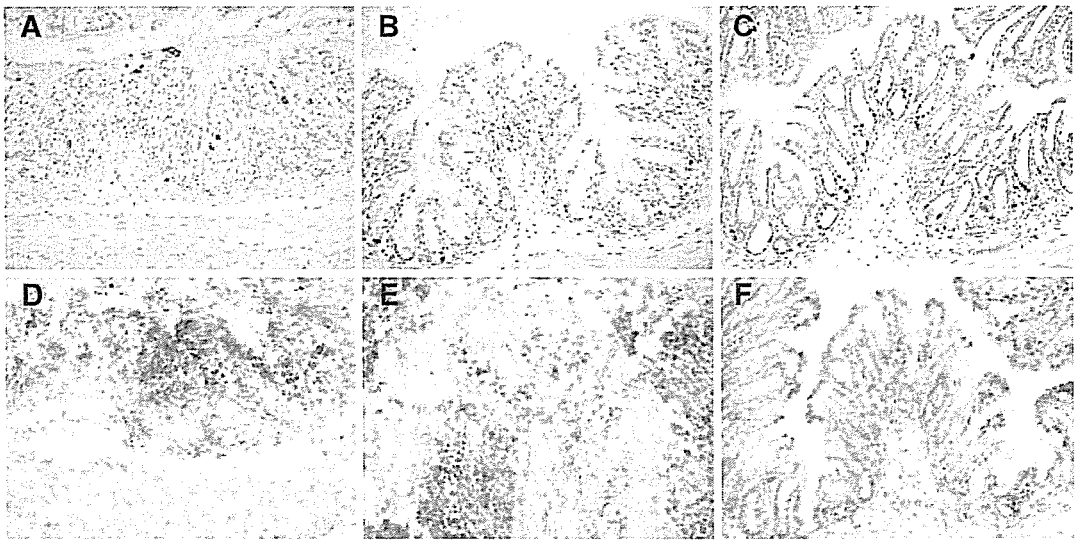

Figure 7. Repeated HGF gene transfection in the liver increasingly promoted proliferation and anti-apoptosis of epithelial cells of the colon. (A–C) BrdU staining of distal-colon tissues from a control pCAGGS-injected mouse (A), from a pCAGGS-HGF mouse injected once (B), and from a pCAGGS-HGF mouse injected twice (C). (D–F) TUNEL staining of the distal-colon tissues from a pCAGGS-injected mouse (D), from a pCAGGS-HGF mouse injected once (E), and from a pCAGGS-HGF mouse injected twice (F)

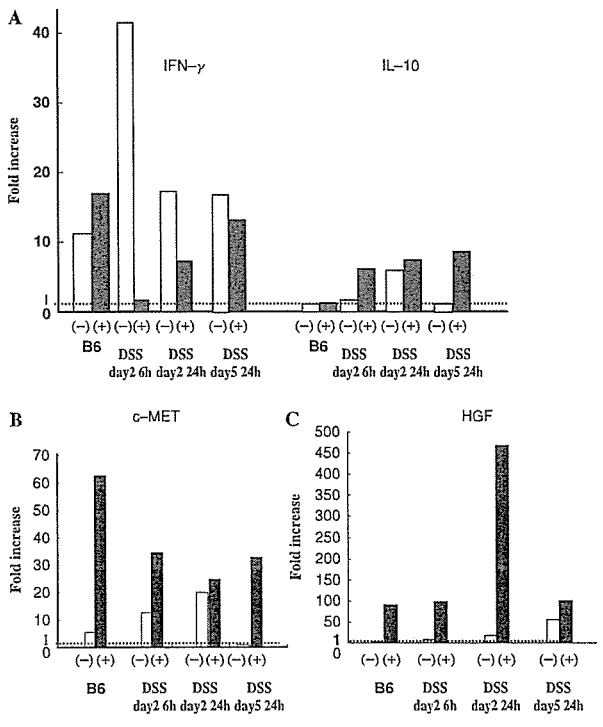

Figure 8. HGF directly regulated the expression of mRNA with decrease for IFN-γ and increase for IL-10 in *ex vivo* colonic tissue culture of mice with DSS colitis. Real-time quantitative PCR of mRNA expression for pro-inflammatory IFN-γ (A), anti-inflammatory IL-10 (A), c-Met (B), and mouse endogenous HGF (C) in the *ex vivo* colon tissue cultured with HGF. The colonic explant samples were taken from mice with DSS colitis on day 2 and day 5, or from those without DSS colitis. The explants were cultured in an organ culture dish for 6 h and 24 h. Open bars, from pCAGGS-injected mice; closed bars, pCAGGS-HGF-injected mice. Each amount was normalized to the level of GAPDH and the final relative values were expressed relative to the calibrators on day 0

Among the alternative methods, naked DNA-mediated gene transfer is the simplest, and techniques for introducing naked DNA into hepatocytes have been the most intensely studied methods for generating therapeutic amounts of gene product [23,24]. Liver-targeted gene transfer is an important tool for expanding the treatment options for diseases of several organs, as well as the liver, because the liver has a great capacity to synthesize serum proteins and is involved in numerous genetic and acquired diseases [29,30]. In this study, we used hydrodynamics-based gene transfer by tail vein injection to transfect the rat HGF gene into hepatocytes to over-express HGF in serum [31–33]. An important feature of the method is that it can achieve liver-targeted gene transfer with naked DNA that is driven by strong, non-tissue-specific, viral promoters, such as the CAG promoter [34].We could effectively transfect the HGF gene into the liver (Figure 1), and induce an ideal elevation of serum HGF levels using this method (Figures 1 and 5). Over-expression of HGF by gene transfer into the liver is an effective method for HGF production, reaching the target organ, the colon, and acting as a drug to ameliorate DSS colitis (Figure 2).

Liver-targeted gene transfer by tail vein injection has a high efficacy, but results in an accelerated decline in gene expression levels (Figure 1) compared with transfer into the muscles of mice by electroporation of the HGF gene *in vivo*. One of the mechanisms of this decline might be an immune response by the mice to the foreign protein, rat HGF. To solve this problem, we injected naked DNA twice, and succeeded in maintaining an elevated serum level of HGF (Figure 5). However, prolonged serum elevation of HGF might have unpredicted side effects on the body such as carcinogenesis [35]. Therefore, we should search for a local method of induction of naked DNA into the intestine, which could exert its therapeutic effects for the

treatment of IBD only in the colon, without increasing the serum HGF level.

This study demonstrated that (1) pretreatment with HGF gene therapy ameliorated the clinical symptoms of DSS colitis; (2) over-expressed HGF in serum ameliorated DSS colitis lesions, associated with an increase of BrdU-positive crypt epithelial cells, and decrease of apoptotic epithelial cells in the colonic crypts of DSS mice; (3) elevated serum HGF inhibited immune cell trafficking into the colon, and suppressed the pro-inflammatory response of DSS colitis; (4) these therapeutic effects of HGF depended on the duration of elevated serum HGF levels; and (5) HGF directly regulated the expressions of mRNA of IL-10 and IFN-γ in colonic explants from mice with DSS colitis.

HGF modulates intestinal epithelial proliferation and migration, serving as a critical regulator of intestinal wound healing, and several studies have reported that this growth factor is useful for the treatment of inflammatory bowel disease. Tahara *et al.* reported that administration of recombinant human HGF released by intraperitoneally transplanted osmotic pumps ameliorated DSS colitis in the rat [20]. Arthur *et al.* also reported that HGF administration by the same method ameliorated diarrhea and colitis in HLA-B27 transgenic rats [21]. Our gene therapy with HGF ameliorated DSS colitis clinically and pathologically through elevation of serum HGF (Figure 2). This could be an alternative drug-delivery method for recombinant HGF treatment of inflammatory bowel disease.

Epithelial repair is immediately accompanied by an immediate inflammatory reaction, and epithelial stem cells are induced to enter DNA synthesis as a result of wounding. HGF has been found to stimulate epithelial proliferation in the lung, stomach, and liver as well as the intestine. We have shown here that HGF gene transfer increased the numbers of BrdU-positive epithelial cells following acute DSS-induced colon injury. This might have caused rapid epithelial regeneration, as demonstrated by histological analysis showing typical regenerative changes and by higher number of surviving crypts compared with untreated mice (Figures 2 and 4).

In addition to its mitogenic activity, HGF has anti-apoptotic properties, and several reports revealed that recombinant HGF therapy ameliorated experimental colitis partially by inhibiting apoptosis of colonic epithelial cells. In this study HGF gene therapy decreased TUNEL-positive colonic epithelial cells in DSS colitis (Figure 4).

In the majority of tissues, HGF is secreted from mesenchymal cells, such as fibroblasts, and its receptor, c-Met, is found typically on epithelial cells. In our study, weak c-Met expression was observed in the crypt epithelial cells in DSS colitis, in both the pCAGGS-injected and pCAGGS-HGF-injected groups (Figure 1). Expression of c-Met mRNA was higher in the DSS colitis group injected with pCAGGS and marginal in the DSS colitis group injected with pCAGGS-HGF (unpublished observation). In the murine model of TNBS colitis, HGF gene transfer into the muscle showed an increased c-Met expression in the colon of untreated mice than those of treated mice, but phosphorylated c-Met expression was stronger in the colon of mice after HGF gene therapy than in untreated mice [36]. We are now investigating the expression of c-Met and its phosphorylation in the colons of mice with HGF gene therapy.

This study demonstrated that HGF gene therapy reduced inflammatory cell trafficking into the colon and suppressed the expression of inflammatory cytokines (Figure 3). In DSS colitis, the first insult of colonic injury is epithelial damage by DSS, resulting in destruction of the gut barrier and influx of intestinal bacterial toxins, and then the inflammatory cascade follows. HGF exerts its mitogenic and anti-apoptotic activity primarily, and thereby restores the gut barrier, leading to a reduction in the infiltration of inflammatory cells and the production of inflammatory cytokines [37,38]. Thus, the anti-inflammatory effect of HGF on DSS colitis might be the secondary effect of HGF in amelioration of DSS colitis. Interestingly, this study showed that expression of the mRNA of the anti-inflammatory cytokine IL-10 is increased markedly in mice with DSS colitis and injected with pCAGGS-HGF (Figure 3). We also observed that the numbers of IL-10-positive cells were not changed in the colons of mice with DSS colitis after HGF gene therapy (unpublished observation). These results might suggest that HGF augments the anti-inflammatory response in the inflamed colon, not by secondary effect but by its own primary effect. To address the point, we performed *ex vivo* organ culture experiments, which revealed the direct effect of HGF on immune response in the colon. We analyzed the expression of mRNA of IFN-γ and IL-10 in the colonic explants of mice with DSS colitis. In the colonic explants of mice with DSS colitis, the levels of expression of the mRNA for the pro-inflammatory cytokine IFN-γ were increased (Figure 8). The expression of mRNA for IFN-γ was clearly reduced by the treatment with HGF on explants (Figure 8), whereas expression of mRNA of IL-10 was increased markedly in the *ex vivo* colon tissue cultured with HGF (Figure 8). Thus, it is likely that HGF directly regulates the transcription of pro-inflammatory and anti-inflammatory cytokines in the diseased colonic tissue. Interestingly, the expression of mRNAs for intrinsic mouse HGF and c-Met was clearly increased in explants cultured with HGF (Figure 8).

However, the present study has not yet revealed the target cells of the HGF in the colon tissue, especially in the context of the anti-inflammatory effect of HGF. In a future study, we should identify the target cells of HGF and the molecular mechanism of how such regulation of cytokine expression works through the stimulation of c-Met, the receptor for HGF, using methods such as reporter gene expression assay.

Finally, our study showed that these therapeutic effects of HGF described above depended on the duration of elevated serum HGF level (Figures 5–7). As mentioned above, repeated injection of the HGF gene solved the problem of a short duration of response following a single injection (Figures 1 and 5). In our previous report, we